# Risk Analysis and Hedging of Parisian Options under a Jump-diffusion Model

Kyoung-Kuk Kim[*] Dong-Young Lim[†]

*Korea Advanced Institute of Science and Technology*

Sept 2015

**Abstract**

A Parisian option is a variant of a barrier option such that its payment is activated or deactivated only if the underlying asset remains above or below a barrier over a certain amount of time. We show that its complex payoff feature can cause dynamic hedging to fail. As an alternative, we investigate a quasi-static hedge of Parisian options under a more general jump-diffusion process. Specifically, we propose a strategy of decomposing a Parisian option into the sum of other contingent claims which are statically hedged. Through numerical experiments, we show the effectiveness of the suggested hedging strategy.

KEYWORDS: Parisian option; risk analysis; dynamic hedging; static hedging

## 1 Introduction

Since the introduction of the barrier option, its rapid development has been observed in over-the-counter markets. Additionally, a number of variants such as partial barriers or double barriers have been created. However, in recent years, the growth of barrier options has slowed down compared to the fast growth in the early 2000's (see, for example, the report on the Bank for International Settlements [2015] which documents the overall market movements). Nonetheless, new financial innovations related to barrier options continue to be introduced as shown in Lei [2014]. A Parisian option is also a barrier-type option in which its payment is activated (or deactivated) only if the underlying asset consecutively remains below (or above) a given barrier over a certain amount of time, namely the option window, specified in the contract. In another variant called Parasian option, its trigger is activated when the total time of the underlying asset below (or above) the barrier is longer than the option window.

[*]Industrial and Systems Engineering, E-mail: kkim3128@kaist.ac.kr

[†]Corresponding author, Industrial and Systems Engineering, E-mail: ldy1848@kaist.ac.kr

In addition to the probabilistically interesting trigger feature, Parisian options have attracted the attention of academics and investors for practical reasons. Suppose that the underlying asset price is getting close to the barrier level. It still is not enough to substantially change the value of a Parisian option whereas barrier options are very sensitive to such a case. This latter characteristic makes the investors of barrier options vulnerable to possible stock price manipulations which could result in unjust profits or losses. The embedded structure of Parisian options thus prevents market players from participating in such deliberate actions [Chesney et al., 1997].

The pricing of Parisian options has been a subject of intense academic scrutiny. Well-known pricing techniques include the Laplace transform approach, partial differential equations (PDEs), lattice models, and so on. Haber et al. [1999] and Avellaneda and Wu [1999] examined numerical solutions obtained from PDEs and lattice models. Chesney et al. [1997] provided a semi-closed form of the option price with the Laplace transform. However, their papers do not discuss the case in which the Brownian excursion is in progress; it was later augmented by Schröder [2003] and Labart and Lelong [2009]. Recently, a recursive method was designed by Dassios and Lim [2013]. While almost all work on pricing has been done under the Black-Scholes model, there is a new development in Albrecher et al. [2012] where the authors extended the pricing formulae to the double exponential jump-diffusion model proposed in Kou [2002]. In addition, exotic types of Parisian options have been studied as well. For example, see Dassios and Wu [2011], Dassios and Lim [2014], Anderluh and van der Weide [2009], Chesney and Gauthier [2006], and Chen and Suchanecki [2011] for the pricing of double-barrier Parisian, two-sided Parisian, American Parisian and Parisian exchange options. Lastly, there is also relevant literature on the excursion times of Parisian type in the context of Lévy insurance models. See Czarna and Palmowski [2011], Loeffen et al. [2013] who derived ruin probabilities when there is a Parisian time delay in realizing ruin for a risk process governed by spectrally negative Lévy processes with sample paths of bounded or unbounded variation.

In contrast to the large number of studies on pricing, there are only a few studies on the hedging of Parisian options. The complicated trigger feature of Parisian options indeed poses a great challenge for hedging. Even the option sensitivities with respect to model parameters have not been fully studied.[1] The rare instances are Haber et al. [1999] and Bernard et al. [2005]; these authors studied the delta and gamma of Parisian options based on PDEs or Laplace transforms.[2] In this paper, we contribute to the existing literature by investigating effective hedging strategies for Parisian options. The simple but widely adopted delta hedging strategy is shown in a later section to result in huge hedging failures. Motivated by this exercise, possible static hedging strategies are proposed and tested in this study. Our underlying approach is based on a method by Nalholm and Poulsen [2006] who unified two popular streams of hedging methods; the first method is by Carr and his co-authors [Bowie and Carr, 1994, Carr and Chou, 1997, Carr et al., 1998], and the second method is by Derman et al. [1995].

The core idea is that we represent the Parisian option value in terms of the prices of other exotic contingent claims, and static hedging strategies are devised for those contingent claims. Specifically, in this study, we will utilize exotic options that are of down-and-in barrier type, up-and-in barrier type, and up-and-out partial barrier type. In addition, all numerical studies are conducted by assuming that the underlying asset dynamics is the double exponential jump-diffusion model; nonetheless, the approach taken in this work can be extended to more general asset dynamics as long as the relevant pricing engines are available. To implement both the dynamic and static hedging methods, one has to have suitable formulae for the Parisian option prices and sensitivities as well as for the vanilla and binary option prices. Such information can be found in the supplement, part of which is a new and meaningful contribution because a more thorough understanding of option sensitivities is indispensable due to their direct implications on risk management activities.

This paper is organized as follows. Section 2 briefly reviews the valuation of Parisian options under the Kou model for which the asset price follows double exponential jump-diffusion dynamics. Section 3 presents dynamic delta hedging in the Black-Scholes model as a motivating example. In Section 4, we devise a quasi-static hedging strategy and compare it with dynamic hedging in Section 5. We conclude in Section 6.

## 2 Review of Parisian options

In this section, we briefly review the definition of Parisian options and the asset dynamics under consideration. There are eight different types of Parisian options, as with standard barrier options, namely down-and-in call/put, down-and-out call/put, up-and-in call/put, and up-and-out call/put. However, it is well documented by Chesney et al. [1997] in Section 4.2 that the 'out' options can be followed from the 'in' case because the sum of one 'out' and one 'in' is just a standard European option. In addition, Section 6 of Chesney et al. [1997] explains how Parisian puts are written in terms of Parisian calls. Hence, without loss of any generality, we focus on Parisian down-and-in call options in this paper.

The risk-neutral dynamics of the underlying asset is a jump-diffusion model given by

$$S_t = S_0 \exp\left(\mu t + \sigma B_t + \sum_{i=1}^{N_t} Y_i\right) \tag{1}$$

where $B_t$ is a standard Brownian motion, $N_t$ is an independent Poisson process with the rate $\lambda$, and $Y_i$'s are i.i.d. random variables. More precisely, $Y_i$ has the density

$$\mathsf{P}(Y_1 \in dy) = p\eta_1 e^{-\eta_1 y}\mathbf{1}_{\{y\geq 0\}}dy + q\eta_2 e^{\eta_2 y}\mathbf{1}_{\{y<0\}}dy$$

with $\mathsf{P}(Y_1 \geq 0) = p = 1 - q$ and $\eta_1, \eta_2$ positive and negative jump rates. The martingale condition on the discounted asset price $\{e^{-rt}S_t\}$ yields

$$\mu = r - \frac{1}{2}\sigma^2 + \lambda\left(1 - p\frac{\eta_1}{\eta_1 - 1} - q\frac{\eta_2}{1+\eta_2}\right).$$

Here, $r$ is the risk-free rate and $\sigma$ is the constant volatility of the underlying asset. See Albrecher et al. [2012] for further information on the underlying model. Note that $\lambda = 0$ or $\eta_1 = \eta_2 = 0$ leads to the Black-Scholes model.

Unlike barrier down-and-in calls, it is necessary to keep track of the accumulated excursion time of the stock price because the stock price needs to stay for a fixed amount of time, denoted as *option window* $D$, below the barrier $L$ for the option to be knocked-in. Thus, we introduce the most important quantity $H_{L,t}$. It is defined as the first time that the excursion time of the asset price below $L$ reaches the knock-in requirement $D$, that is, $H_{L,t} = \inf\{s \geq t | s - g_s \geq D\}$ where $g_u = \sup\{s \leq u | S_s \geq L\}$.[3] Hence, the option feature becomes active if and only if $H_{L,t} \leq T$. This is equivalent to the condition in which there exists some $a$ such that $S_t < L$ for all $t \in (a, a + D) \subset [0, T]$ [Schröder, 2003].

Due to this knock-in requirement, special care must be taken depending on whether the current stock price is above or below the barrier. Because we need to take into account the accumulated excursion time if the current stock price, say $S_t$, is below the barrier, we introduce an additional parameter, *remaining window* $d \in [0, D]$. In this case, one can see that the random variable $H_{L,t}$ depends on $S_t$ and $d$, not on the whole history of the asset price. Then, the risk neutral pricing formula tells us that the Parisian call price at time $t$ is

$$\mathfrak{C}_t(S_t, d; \Theta) = e^{-r\tau} \mathsf{E}_t \left[ \mathbf{1}_{H_{L,t} \leq T} \left\{ S_t \exp\left( \mu\tau + \sigma B^*_\tau + \sum_{i=1}^{N^*_\tau} Y_i \right) - K \right\}^+ \right] \tag{2}$$

where $\tau = T - t$ is the time-to-maturity and $\Theta$ refers to other contract parameters $\{T, L, K, D\}$. The subscript $t$ means the conditional expectation given the information, say $\mathcal{F}_t$, at time $t$. Additionally, $B^*_s = B_{t+s} - B_t$ and $N^*_s = N_{t+s} - N_t$ are a standard Brownian motion and a Poisson process independent of $\mathcal{F}_t$, respectively. We note that the right hand side of the above pricing formula implicitly depends on the parameter $d$ via $H_{L,t}$.

In order to implement the hedging strategies considered in this paper, formulae for prices and sensitivities (or greeks) are essential. As briefly summarized earlier, the valuation of Parisian options can be found in, e.g., Chesney et al. [1997], Schröder [2003], Labart and Lelong [2009], or Albrecher et al. [2012]. On the other hand, the delta and gamma of Parisian options under the Black-Scholes model (with no excursions) are computed in Bernard et al. [2005] with the Laplace transforms. Since such treatments of greeks are limited as explained in the introduction, we provide additional but necessary formulae for the option prices and sensitivities under the Black-Scholes model as well as (1) in the supplement. Some of the formulae appear to be new in the literature.[4]

# 3 Motivating Example

## 3.1 Dynamic hedging under the Black-Scholes dynamics

Dynamic delta hedging, or more generally hedging based on portfolio immunization, is an important method of managing risks inherent in financial derivatives. Although a perfect replication is possible in an ideal setting, practical limitations such as discrete re-balancing have raised concerns about dynamic hedging. As a motivating example, we consider dynamic delta hedging for Parisian options under the Black-Scholes model and investigate how and why such hedging operations might result in unsatisfactory outcomes. Particular attention is given to the so called *cushion effect*, which means that a Parisian option is relieved from undesirable problems generated by abrupt changes in payoff values when the underlying asset breaches the barrier [Schröder, 2003, Albrecher et al., 2012].

Details on the hedging operations are deferred to the section on the numerical results. Here, we simply denote the delta hedging errors by $\mathsf{HE}$ (relative to the initial option price in the absolute value) and measure the hedging performance by adopting two popular risk measures, value-at-risk (VaR) and expected shortfall (ES), given as

$$\mathrm{VaR}_\alpha(\mathsf{HE}) = \inf\Big\{l \in \mathbb{R} \mid \mathsf{P}(\mathsf{HE} > l) \le \alpha\Big\}, \quad \mathrm{ES}_\alpha(\mathsf{HE}) = \mathsf{E}\Big[\mathsf{HE} \mid \mathsf{HE} \ge \mathrm{VaR}_\alpha(\mathsf{HE})\Big]$$

where $\alpha$ is a user-defined level, typically 10% or 5%. Relevant parameters in (1) and (2) are specified in Table 1.[5]

Table 1: Parameter values used in hedging experiments.

| $r$ | $\sigma$ | $T$ | $K$ | $L$ | $S_0$ | $D$ | $p$ |
|---|---|---|---|---|---|---|---|
| 0.05 | 0.2 | 1 | 95 | 90 | 91 | 0.2 | 0.3 |

Table 2: Mean, value-at-risk, and expected shortfall of simulated $\mathsf{HE}$ with parameter values in Table 1 and sample size 1000.

| risk measure / # of time steps | mean | $\mathrm{VaR}_{0.1}$(%) | $\mathrm{ES}_{0.1}$(%) | $\mathrm{VaR}_{0.05}$(%) | $\mathrm{ES}_{0.05}$(%) |
|---|---|---|---|---|---|
| 120 | 35.94 | 82.78 | 163.05 | 125.50 | 225.90 |
| 240 | 26.77 | 63.25 | 120.87 | 92.77 | 166.16 |
| 480 | 19.73 | 46.92 | 89.67 | 65.92 | 124.05 |
| 2400 | 10.88 | 24.01 | 56.43 | 36.14 | 82.76 |

The results of the hedging simulation are summarized in Figure 1 and Table 2. The histogram of $\mathsf{HE}$ for portfolio re-balancing approximately twice a day is shown in the figure, from which we observe that most

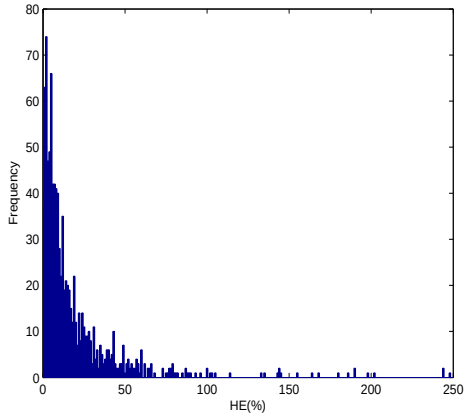


Figure 1: Histogram of simulated HE with parameter values in Table 1, time steps 480, and sample size 1000.

of the outcomes are less than 50% but it could be as large as 250%. On the other hand, VaR and ES together with the mean HE are listed in the table for four different hedging frequencies. Even when the number of time steps is 2400, which corresponds to approximately 10 hedging operations a day, the 5%-level VaR and ES come close to 36% and 82%. Such a slow decrease in the hedging errors is indeed a systematic behavior when dealing with complex payoffs [Gobet and Temam, 2001]. A more careful look into the path-by-path performance reveals that large errors could occur due to massive hedging failures in some of the simulated scenarios.

For a better understanding, let us consider two particular asset paths in Figures 2(a) and 3(a). In the former, the underlying asset never touches the barrier $L$ during the life time of the option. In such a case, the option prices and greeks do not have excessive fluctuations and delta hedging works well. Figure 2(b) shows the cumulative hedging errors which converge to 0.005 in an absolute scale. On the other hand, in Figure 3(a), the option is knocked-in at time 0.23 (the 92th time step). For the same path, Figure 3(b) shows the cumulative hedging errors for the Parisian call.[6] Similar information for a vanilla call is shown in Figure 3(c). Note that the cumulative hedging error for the Parisian call at time 0.23 is over 1.5 whereas it is -0.1317 for the vanilla call. This difference is more prominent if we normalize them by the initial option prices, yielding 208.99% and -1.75%, respectively.

### 3.2 Sensitivity analysis

Recall that a delta-hedged portfolio, say $\pi_t$, is structured with a target option and shares of stocks[7] in a way that the portfolio has zero first order sensitivities with respect to the movement of stock price $\delta S_t$ over a

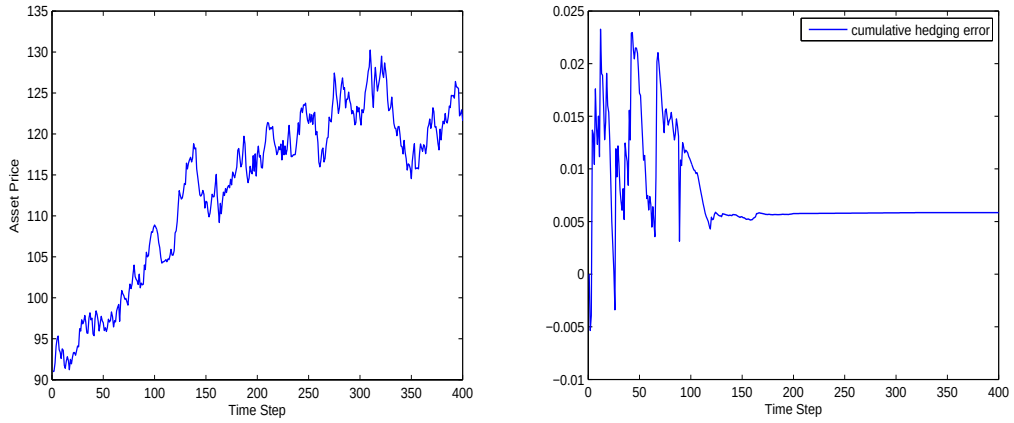


(a) Path of underlying asset

(b) Cumulative hedging error

Figure 2: Delta hedging of a Parisian down-and-in call with parameter values in Table 1.

short period of time $\delta t$. The resulting difference in the portfolio values can be written as

$$\delta\pi_t = \pi_{t+\delta t} - \pi_t = \frac{1}{2}\Gamma_t(\delta S_t)^2 + \theta_t \delta t + o\left(\delta t\right)$$

where $\Gamma_t$ is gamma and $\theta_t$ is theta. The last term means that the remaining errors have a smaller magnitude than $\delta t$.

This relationship immediately shows that large gamma or theta values might lead to large errors. For example, the effect of theta or the contribution of theta $\theta_t \delta t$ on hedging errors is shown in Figure 3(b) for the scenario in Figure 3(a). This result is in stark contrast with the vanilla call case in Figure 3(c). It is particularly interesting that the theta values have big spikes as the asset price path fulfills the knock-in requirement.

The theta of Parisian options is somewhat peculiar in the sense that two sources of changes need to be considered when the excursion is in progress. In such a case, decreasing the time-to-maturity as well as the remaining window affects the option value; thereby yielding the expression $\theta_t = \theta_\tau + \theta_d$ where $\theta_\tau = -\partial\mathfrak{C}/\partial\tau$ and $\theta_d = -\partial\mathfrak{C}/\partial d$. Figure 4 shows a comparison of the theta values for the Parisian, barrier, and vanilla calls. One can notice that the Parisian thetas are relatively large and they are more so for smaller $d$ values, i.e., close to knock-in.

The situation can worsen due to the gamma values. Actually, as shown in Figure 5(a), a larger option window $D$ results in less fluctuating delta curves and thus smaller gamma values, proving the existence of the cushion effect. This is not like in barrier options which exhibit delta curves with heavy swings near the barrier. What is missing in Figure 5(a), however, is whether the same thing happens when the excursion is in progress. Part (b) of Figure 5 illustrates that this is not the case; in fact, such behaviors increase as $d$ gets smaller. Therefore, it becomes clear that a hedger of a Parisian option cannot enjoy the cushion effect in practice.

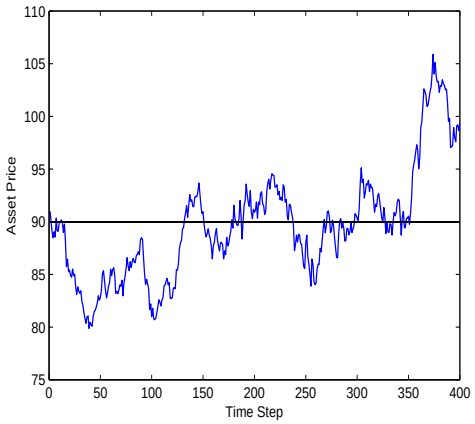


(a) Path of underlying asset

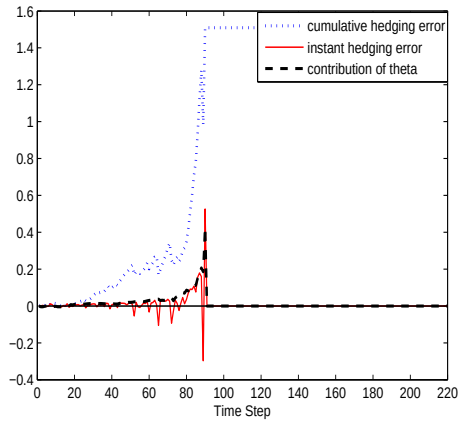


(b) Parisian option

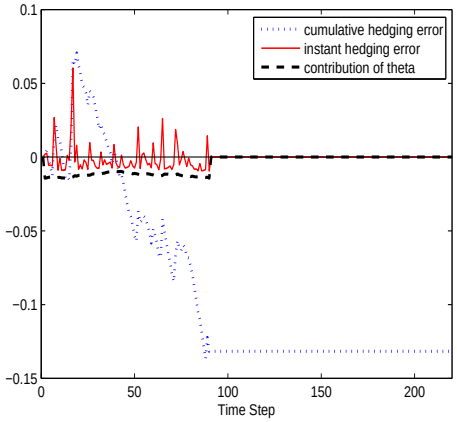


(c) Vanilla option

Figure 3: Delta hedging of a Parisian down-and-in call and a vanilla call with parameter values in Table 1.

Portfolio immunization using higher order sensitivities with additional market instruments could be an alternative way of reducing significant hedging failures. However, its effectiveness is still questionable, especially if the asset price dynamics has jumps as described in (1). To tackle such deficiencies in dynamic delta hedging, other approaches have been proposed and tested in the literature. Among the many methods, two successful and widely adopted methods were systemically investigated by Derman et al. [1995] and Carr et al. [1998]. Although barrier type options have been discussed extensively in the literature, the existing methods are not directly applicable to Parisian options due to their special trigger feature. This problem is resolved in the next section.

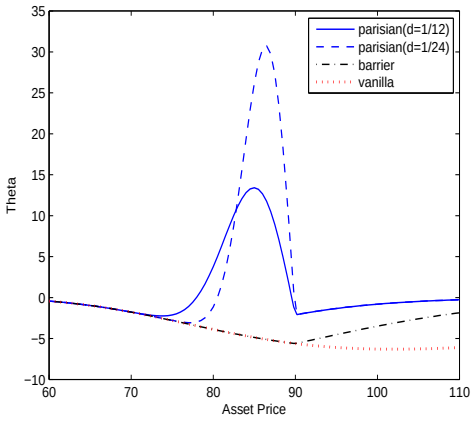


Figure 4: Theta curves of down-and-in Parisian, down-and-in barrier and vanilla call with the same strike and the barrier level: $D = 2/12$ and other parameter values in Table 1.

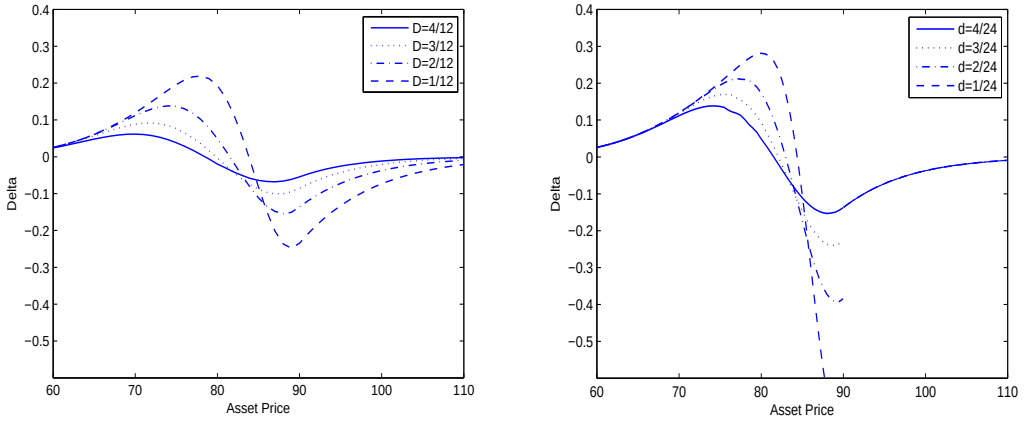


(a) $d = D$ (b) $D = 2/12$

Figure 5: Delta curves of down-and-in Parisian call option for various $d$ and $D$ with parameter values in Table 1.

# 4 Construction of Static Hedges

## 4.1 Decomposing Parisian options

Static or quasi-static hedges have received much attention from practitioners and from academics. Such approaches are particularly beneficial when dynamic hedges do not produce practically meaningful results or when one is concerned with model misspecification. Sometimes model-free suboptimal hedges provide upper or lower bounds of a given contingent claim. In the literature, one popular method was developed by Bowie and Carr [1994] and Carr et al. [1998]. It utilizes vanilla options with different strike prices but with the same maturity to replicate target options. The key idea is the symmetry of European claims. This

Table 3: Relevant contingent claims that appear in quasi-static hedging operations.

| symbol | description ($\Theta = \{T, L, K, D\}$) |
|---|---|
| $\mathfrak{C}_t^{\mathrm{bin}}(x;T,K)$, $\mathfrak{P}_t^{\mathrm{bin}}(x;T,K)$ | cash-or-nothing binary call and put options |
| $\mathfrak{B}_t^{\mathrm{d\cdot i}}(x,T_1;\Theta)$, DIB | down-and-in barrier-type option with payoff $\mathfrak{C}_{t^*}(S_{t^*},D;\Theta)$ at $t^*$ only if $L$ is breached at $t^*$ and $t^* < T_1$ |
| $\mathfrak{B}_t^{\mathrm{u\cdot i}}(x,T_1;\Theta)$, UIB | up-and-in barrier-type option with payoff $\mathfrak{C}_{t^*}(S_{t^*},D;\Theta)$ at $t^*$ only if $L$ is breached at $t^*$ and $t^* < T_1$ |
| $\mathfrak{B}_t^{\mathrm{u\cdot o\cdot partial}}(x,T_1;\Theta)$, UOPB | up-and-out partial barrier call which expires worthless if $t^* < T_1$, otherwise, it turns into a vanilla call with maturity $T$ and strike $K$ |

is called the *strike-spread approach* in the literature. On the other hand, Derman et al. [1995] proposed a method of replicating target options by using vanilla options with different maturities but with the same strike. For example, a barrier option can be hedged by vanilla options with a strike equal to the barrier level so that replication is done at the barrier as well as at the expiry. One notable advantage of this so called *calendar-spread approach* is that it provides a model-independent hedging strategy. Recently, Chung and Shih [2009] and Chung et al. [2013] studied pricing and static hedging of American (knock-in) options under the CEV model.

One of the most thoroughly studied options from a static hedging viewpoint is barrier options. Hedging instruments include vanilla options, binary options, etc. see Chung et al. [2010] and references therein. Although Parisian options are a variant of barrier options, the hedging strategies developed for barrier options are not directly applicable to Parisian options. For most types of barrier options studied so far, the knock-in (or knock-out) boundaries are depicted on the $(t, S_t)$-plane. However, this is no longer the case for Parisian options, and this additional complexity requires special treatment.

The central idea of our approach is to decompose a Parisian option into other contingent claims for each of which a static hedging strategy can be devised. For this purpose, we first fix some notation. The European call price is denoted as $\mathfrak{C}_t^{\mathrm{E}}(x;T,K)$ where $x$ is the current stock price, $K$ the strike, $T$ the maturity, and the current time as $t$. Similarly we define $\mathfrak{P}_t^{\mathrm{E}}(x;T,K)$ the corresponding European put option.[8] Furthermore, $\mathfrak{C}_t(x,d;\Theta)$ with $\Theta = \{T, L, K, D\}$ denotes the Parisian option price at time $t$. We list other relevant contracts in Table 3. Here a partial barrier option refers to a barrier-type contract such that a barrier ceases to exist at some time before the option maturity. The two exotic contracts $\mathfrak{B}^{\mathrm{d\cdot i}}$ and $\mathfrak{B}^{\mathrm{u\cdot i}}$ have an early-redemption feature, that is, the contract returns the payoff at $t^*$ with no further cash exchange.

**Proposition 1** *Consider a Parisian down-and-in call $\mathfrak{C}_t(x,d;\Theta)$ with $\Theta = \{T, L, K, D\}$. Then, the following relationships hold.*

1. *<u>case $x > L$</u>: (effectively $d = D$) for $0 \leq t < T$,*

$$\mathfrak{C}_t(x, d; \Theta) = \mathfrak{B}_t^{\mathrm{d\cdot i}}(x, T - d; \Theta); \tag{3}$$

2. *<u>case $x < L$</u>: for $0 \leq t < T - d$,*

$$\mathfrak{C}_t(x, d; \Theta) = \mathfrak{B}_t^{\mathrm{u\cdot i}}(x, \min\{t + d, T - D\}; \Theta) + \mathfrak{B}_t^{\mathrm{u\cdot o\cdot partial}}(x, t + d; \Theta). \tag{4}$$

**Proof:** <u>*case 1.*</u> Let $t^*$ be the first hitting time of the barrier $L$ after $t$. Suppose $t^* < T - D = T_1$. Then, it is easy to see that the down-and-in option pays off $\mathfrak{C}_{t^*}(S_{t^*}, D; \Theta)$[9] which is exactly the Parisian option price at $t^*$. Suppose $t^* \geq T - D$. Then, both options expire worthless.

<u>*case 2.*</u> Now assume that the current stock price is below $L$ with remaining window $d$. Suppose that the asset price remains below $L$ during $[t, t + d)$ or simply $t^* \geq t + d$. Then, the Parisian option has the value $\mathfrak{C}^{\mathrm{E}}_{t+d}(S_{t+d}; T, K)$ at time $t + d$. On the other hand, the up-and-in option expires worthless because $t^* > \min\{t + d, T - D\} = T_1$. However, the trigger for the up-and-out option is not activated and the partial barrier disappears, making its value equal to $\mathfrak{C}^{\mathrm{E}}_{t+d}(S_{t+d}; T, K)$ at time $t + d$.

Suppose the stock price hits $L$ at $t^* < t + d$. If further $t^* < T - D$, then the remaining window of the Parisian option is re-set at $t^*$ and its value is equal to $\mathfrak{C}_{t^*}(S_{t^*}, D; \Theta)$. The up-and-in option is knocked-in and has the payoff $\mathfrak{C}_{t^*}(S_{t^*}, D; \Theta)$ whereas the up-and-out option expires worthless. This equality still holds when $t^* = T - D$ because $\mathfrak{C}_{T-D}(S_{t^*}, D; \Theta) = 0$. Lastly, if $t^* > T - D$, then all the components vanish with remaining values 0. ■

We note that the above result does not utilize any particular feature of the underlying model, hence it should be applicable to more general models with a one-dimensional Markovian structure. From Proposition 1, the task of hedging a Parisian option reduces to hedge $\mathfrak{B}^{\mathrm{d\cdot i}}$ (DIB), $\mathfrak{B}^{\mathrm{u\cdot i}}$ (UIB), and $\mathfrak{B}^{\mathrm{u\cdot o\cdot partial}}$ (UOPB) for which the knock-in/out boundaries are simply the barrier level. Indeed, if three products are statically hedge-able, then one can switch between the hedge portfolios for $\mathfrak{B}^{\mathrm{d\cdot i}}$ and $\mathfrak{B}^{\mathrm{u\cdot i}} + \mathfrak{B}^{\mathrm{u\cdot o\cdot partial}}$ whenever the barrier level is crossed. The simple knock-in/out boundaries for those options enable us to apply existing methods in the literature.

### 4.2 Principles of the unified approach

One stream in the literature on static hedging describes exact hedging methods under asset dynamics with specific structures. However, there is no such formula for our target options (UIB, DIB and UOPB) under the jump-diffusion model (1). The underlying approach we take, thus, is the calendar-spread approach so that model independent static hedging portfolios (SHP) can be constructed. In addition, we utilize the basic insight of the strike-spread approach by constructing so called *expiry hedges*. This combination of the

strike-spread and calendar-spread approaches was introduced by Nalholm and Poulsen [2006] who focused on barrier options and termed expiry hedges. The proposed method by the authors, referred to as the *unified approach*, consists of two steps.

1. Construct an expiry hedge for a target barrier option with the maturity $T$. The selection of an expiry hedge is flexible; Nalholm and Poulsen [2006] examined four different expiry hedges. This portfolio of hedging instruments with the maturity $T$ is designed to mimic the barrier option price at the barrier along the time axis as well as at the maturity $T$.

2. Apply the calendar-spread approach to the remainder. In more detail, we additionally match the value of the SHP and the target option at the barrier level by adding new hedging instruments with different maturities. The amounts of those hedging instruments are determined with a system of certain linear equations.

**Example 1** For an illustration, let us consider an up-and-out barrier option with strike 90 and barrier 95. An expiry hedge with payoff $\Lambda_t(x;T)$ called *the perfect one-sided hedge* by Nalholm and Poulsen [2006] is given by

$$\Lambda_T(x;T) = \mathfrak{C}_T^{\mathrm{E}}(x;T,90) - 5\mathfrak{C}_T^{\mathrm{bin}}(x;T,95) = (x-90)^+ - 5\cdot\mathbf{1}_{\{x\geq 95\}}$$

where $x$ is the stock price at $T$. This matches the barrier option at $T$ exactly, however, this portfolio does not reflect the knock-out possibility at any time $t<T$. Here $\Lambda_t(x;T)$ denotes the time $t$ price of the expiry hedge with an underlying stock price $x$. One better performing expiry hedge given in Nalholm and Poulsen [2006] is *the perfect two-sided hedge*:

$$\Lambda_T(x;T) = \mathfrak{C}_T^{\mathrm{E}}(x;T,90) - \mathfrak{C}_T^{\mathrm{E}}(x;T,100) - 10\mathfrak{C}_T^{\mathrm{bin}}(x;T,95).$$

See Figure 6 for the payoff function at $T$. ∎

**Example 2** One can try to hedge the same barrier option with the calendar-spread approach alone. Consider a given set of time points $t=t_0<t_1<\cdots<t_n=T$. In this case, an SHP at time $t$ can be constructed as a weighted sum of $n$ vanilla calls, for instance,

$$\sum_{i=1}^{n} w_i \mathfrak{C}_t^{\mathrm{E}}(x;t_i,95).$$

Here, $w_i$'s solve

$$\sum_{i=k+1}^{n} w_i \mathfrak{C}_{t_k}^{\mathrm{E}}(95;t_i,95) = 0, \quad k=0,1,\ldots,n-1.$$

The idea behind this construction is as follows. If the underlying asset hits the barrier at one of the time points $t_i$'s, then the target option and the SHP have the same value, zero. If the underlying asset never hits

the barrier until $T$, then the final payoff coincides as well. Hedging errors occur due to the mismatches between the $t_i$'s. ∎

The two examples above show that the expiry hedge and the calendar-spread approach complement each other. Actually, carefully constructed expiry hedges with certain assumptions about asset dynamics can indeed be perfect static hedges as discussed in Bowie and Carr [1994] and Carr et al. [1998] for example. However, in general an expiry hedge is hardly perfect and its choice is made on a case by case basis. And the remaining part not captured by an expiry hedge is covered by a weighted sum of the hedging instruments with different maturities. In the next subsection, we shall construct SHPs for our target options UIB, DIB, and UOPB following these principles. Note that each of these options is not a barrier option but its exotic variant.

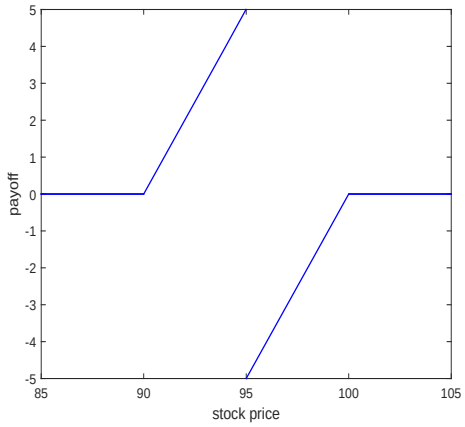


Figure 6: Perfect twosided expiry hedge for an up-and-out barrier call option with strike 90, barrier 95.

### 4.3 Quasi-static hedges

Let us first consider the construction of a static hedge for DIB at a given time $t$ with its value function $\mathfrak{B}_t^{\mathrm{d\cdot i}}(x, T-D; \Theta)$ and $x > L$. We assume that $t < T - D$; otherwise, the Parisian option has a value of 0 and there is no need for hedging with (3). The hedging of DIB is relatively easy compared to that of UIB or UOPB; the latter two belong to a class of reverse barrier options which are difficult to hedge due to the discontinuous payoff feature. Thus, we do not set any expiry hedges for DIB, that is, we set $\Lambda_t(x; T-D) \equiv 0$.

Next, let us fix $n$ and choose a set of points between $t$ and $T-D$, say $t = t_0 < t_1 < \cdots < t_n = T - D$. The hedge portfolio consists of $n$ different put options with the strikes $H_i$:

$$\pi_t^{(n)}\left(x; \mathfrak{B}^{\mathrm{d\cdot i}}\right) = \sum_{i=1}^{n} w_i \mathfrak{P}_t^{\mathrm{E}}(x; t_i, H_i), \quad 0 < H_i \le L \tag{5}$$

where $w_i$'s are the amounts of the put options to be determined shortly. Note that DIB and the above portfolio have a value of 0 if the barrier is never hit until $T - D$. Next, we match $\pi_t^{(n)}$ with DIB at the barrier by choosing the appropriate $w_i$'s with a system of linear equations as follows:

$$\mathfrak{C}_{t_k}(L, D; \Theta) = \sum_{i=k+1}^{n} w_i \mathfrak{P}^{\mathrm{E}}_{t_k}(L; t_i, H_i) = \pi^{(n)}_{t_k}\left(L; \mathfrak{B}^{\mathrm{d\cdot i}}\right), \quad k = 0, 1, \ldots, n-1. \tag{6}$$

We observe that the Parisian option prices and put option prices are readily available. In the matrix form, we only have to solve $Aw = b$ where $A$ is a $n \times n$ upper triangular matrix with its $(i, j)$-th element $a_{ij} = \mathfrak{P}^{\mathrm{E}}_{t_{i-1}}(L; t_j, H_j)$ for $j = i, i+1, \ldots, n$ and $b_i = \mathfrak{C}_{t_{i-1}}(L, D; \Theta)$. The uniqueness of $w$ is guaranteed by the invertibility of $A$. This $n$-point hedging portfolio is approximate in nature because it replicates the option payoff only at finitely many points. However, it is intuitively clear that, by considering more points, the replication becomes the better.

Figure 7(a) compares the option payoff $\mathfrak{C}_s(L, D; \Theta)$ and the 9-point SHP with its value function $\pi_s^{(9)}\left(L; \mathfrak{B}^{\mathrm{d\cdot i}}\right)$, say SHP(DIB), for $0 \le s \le T - D$. The time grid is selected by $t_i = i(T - D)/9$, and all $H_i$'s are set equal to $L$. The right panel shows their differences. If DIB is continuously knocked-in, by construction, the mismatch values are zero at $t_0, \ldots, t_{n-1}$. There is no mismatch even at $t_n$ because both the option value and the portfolio value are zero at that point. If an overshoot occurs across the barrier due to a possible stock price jump, an additional error may arise even at value matching points.

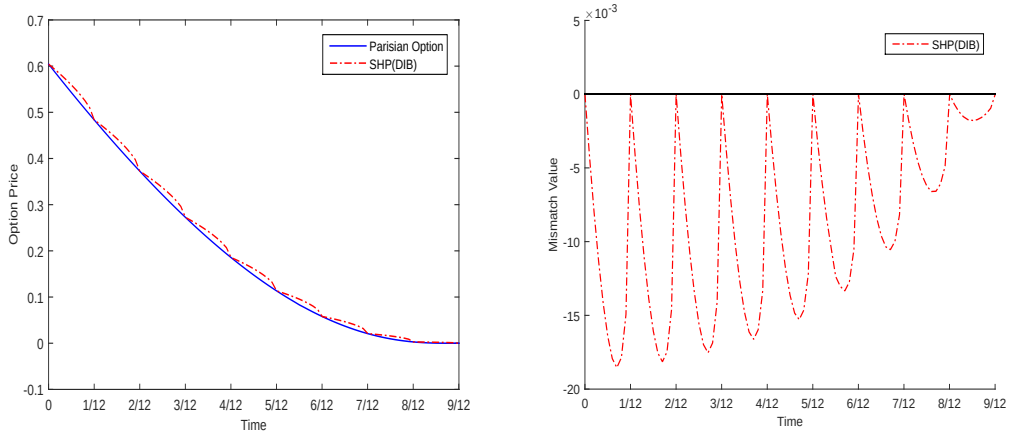


(a) (b)

Figure 7: The value functions of DIB and its 9-point SHP along the barrier $L$ and their differences for $s \in [0, T - D]$; $D = 0.25$, $T = 1$, $\sigma = 0.2$, $r = 0.05$, $\lambda = 3$, $p = 0.3$, $\eta_1 = 50$, $\eta_2 = 50$.

Let us turn our attention to the construction of a static hedge for UOPB at a given time $t$. In this case, we have $x < L$. Still, $d$ denotes the remaining window, and we assume that $t < T - D$ and choose a set of points between $t$ and $t + d$, say $t = t_0 < t_1 < \cdots < t_n = t + d$. Note that our hedging horizon is $t + d$ because the barrier of UOPB exists up to $t + d$ in (4). For an expiry hedge, one can consider the two-sided

expiry hedge as mentioned in the previous example. In this case, however, it turns out to be more effective to consider a slightly modified hedge

$$\Lambda_{t_n}(x;t_n) = \mathfrak{C}^{\mathrm{E}}_{t_n}(x;T,K) - \mathfrak{C}^{\mathrm{E}}_{t_n}(x;t_n,H) - w^{\mathrm{bin}}\mathfrak{C}^{\mathrm{bin}}_{t_n}(x;t_n,L)$$

for some constants $w^{\mathrm{bin}}$ and $H > L$. The constant $w^{\mathrm{bin}}$ can be chosen, for instance, by setting

$$0 = \mathfrak{C}^{\mathrm{E}}_{t_{n-1}}(x;T,K) - \mathfrak{C}^{\mathrm{E}}_{t_{n-1}}(x;t_n,H) - w^{\mathrm{bin}}\mathfrak{C}^{\mathrm{bin}}_{t_{n-1}}(x;t_n,L).$$

In the next step, additional hedging instruments are included in the SHP so that its value function is given as

$$\pi^{(n)}_t\left(x;\mathfrak{B}^{\mathrm{u\cdot o\cdot partial}}\right) = \sum_{i=1}^{n} w_i\mathfrak{C}^{\mathrm{E}}_t(x;t_i,H_i) + \Lambda_t(x;t_n), \quad L \le H_i < \infty.$$

Note that the UOPB expires worthless if the stock price hits $L$ before $t+d$. Hence, we have the following system of linear equations:

$$0 = \sum_{i=k+1}^{n} w_i\mathfrak{C}^{\mathrm{E}}_{t_k}(L;t_i,H_i) + \Lambda_{t_k}(L;t+D), \quad k = 0,1,\ldots,n-1.$$

Lastly, UIB can be similarly handled. We assume that $t < T - D$ and $t = t_0 < t_1 < \cdots < t_n = \min\{t+d, T-D\}$. An expiry hedge is chosen as

$$\Lambda(x;t_n) = w^{\mathrm{bin}}\mathfrak{C}^{\mathrm{bin}}(x;t_n,L), \quad w^{\mathrm{bin}} = \frac{\mathfrak{C}_{t_{n-1}}(L,D;\Theta)}{\mathfrak{C}^{\mathrm{bin}}_{t_{n-1}}(L;t_n,L)}.$$

And our $n$-point SHP is found by

$$\pi^{(n)}_t\left(x;\mathfrak{B}^{\mathrm{u\cdot i}}\right) = \sum_{i=1}^{n} w_i\mathfrak{C}^{\mathrm{E}}_t(x;t_i,H_i) + \Lambda_t(x;t_n), \quad L \le H_i < \infty. \tag{7}$$

Because the UIB has the payoff $C_s(L,D;\Theta)$ along the barrier for $s \in [0,t_n]$, we equate

$$\mathfrak{C}_{t_k}(L,D;\Theta) = \pi^{(n)}_{t_k}\left(L;\mathfrak{B}^{\mathrm{u\cdot i}}\right), \quad k = 0,1,2,\ldots,n-1. \tag{8}$$

For a numerical illustration, see Figure 8 for the case of the UOPB + UIB where $S_0 < L$ and $d = D$. We consider a 6-point SHP with equally divided time steps $t_i = iD/6$. The strikes of all the vanilla options are set at $L$. The left panel compares the value functions of the Parisian option and the SHP along the barrier $L$ for the time interval $[0,D]$. Their differences are shown in the right panel. The dotted curves in the figure show how much additional mismatch values occur if no expiry hedge is taken into account. Such great differences, specially around $D$, are inevitable due to the construction. For instance, the function value $\mathfrak{B}^{\mathrm{u\cdot i}}_s(L,D;\Theta)$ of UIB jumps from $\mathfrak{C}_{D-}(L,D;\Theta)$ to 0 at $s = D$ whereas $\pi^{(6)}_s\left(L;\mathfrak{B}^{\mathrm{u\cdot i}}\right)$ is continuous on $[0,D]$.

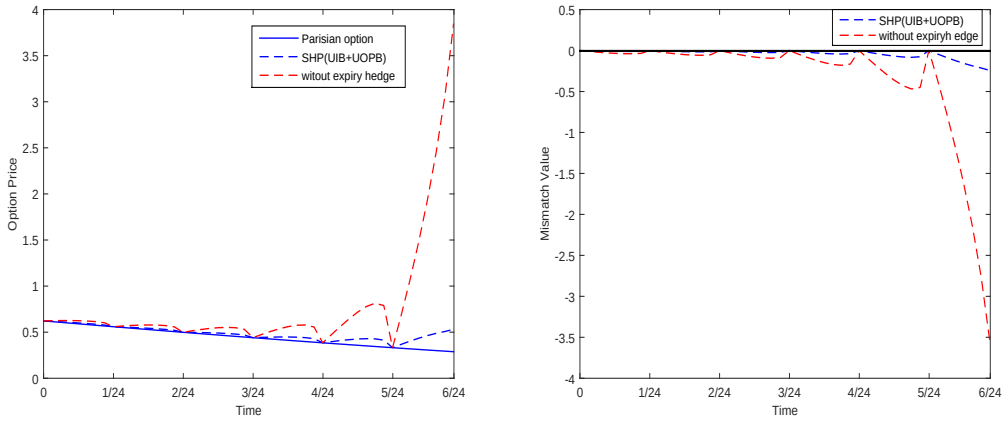


(a) (b)

Figure 8: The value functions of UIB + UOPB and its 6-point SHP along the barrier $L$ and their differences for $s \in [0, D]$; $D = 0.25$, $T = 1$, $\sigma = 0.2$, $r = 0.05$, $\lambda = 3$, $p = 0.3$, $\eta_1 = 50$, $\eta_2 = 50$.

**Remark 1** It is known that, in the calendar-spread approach, a hedge position of reverse barrier type options such as up-and-out calls can be very large as the differences of vanilla option maturities become smaller. In our example in Figures 7 and 8, we explicitly compute the required option positions. As reported in Table 4, their quantities are moderate, and we observed from our experiments that they tend to stay bounded even for smaller differences in the option maturities. This is because the expiry hedge makes the payoffs of the target options smoother than that of the calendar-spread approach. ∎

### 4.4 Additional comments

Previously, it was pointed out that an expiry hedge could be helpful in reducing discrepancies due to the discontinuity of the value functions along the barrier $L$. There is another approach, referred to as *theta matching*, to handle such a problem under continuous asset dynamics. We compare this approach introduced by Chung et al. [2010] with the unified approach in our numerical experiments.

To fix the idea, let us consider the case of UIB. If we include binary options in order to match the thetas of the portfolio and the target option, then the resulting SHP becomes

$$\widetilde{\pi}_t^{(n)}\left(x; \mathfrak{B}^{\mathrm{u\cdot i}}\right) = \sum_{i=1}^{n} w_i \mathfrak{C}_t^{\mathrm{E}}(x; t_i, H_i) + w^{\mathrm{bin}} \mathfrak{C}^{\mathrm{bin}}(x; t_n, L).$$

The relevant weights $w_i$'s and $w^{\mathrm{bin}}$ are determined by the following system of linear equations:

$$\mathfrak{C}_{t_k}(L, D; \Theta) \quad = \quad \sum_{i=k+1}^{n} w_i \mathfrak{C}_{t_k}^{\mathrm{E}}(L; t_i, H_i) + w^{\mathrm{bin}} \mathfrak{C}_{t_k}^{\mathrm{bin}}(L; t_n, L), \quad k = 0, 1, \ldots, n-1, ;$$

Table 4: Static hedging portfolio for DIB and UIB+UOPB under the parameter set of Figures 7 and 8.

| DIB | | | | UIB+UOPB | | | |
|---|---|---|---|---|---|---|---|
| type | quantity | maturity | strike | type | quantity | maturity | strike |
| European put | 0.0302 | 1/12 | 90 | European call | 0.0216 | 1/24 | 90 |
| | 0.0296 | 2/12 | 90 | | 0.0316 | 2/24 | 90 |
| | 0.0285 | 3/12 | 90 | | 0.0497 | 3/24 | 90 |
| | 0.0265 | 4/12 | 90 | | 0.0850 | 4/24 | 90 |
| | 0.0246 | 5/12 | 90 | | 0.1536 | 5/24 | 90 |
| | 0.0211 | 6/12 | 90 | | 0 | 6/24 | 90 |
| | 0.0162 | 7/12 | 90 | | 1 | 6/24 | 95 |
| | 0.0091 | 8/12 | 90 | binary call | 10.6384 | 6/24 | 90 |
| | 0.0016 | 9/12 | 90 | | | | |

$$\theta_{t_{n-1}}(L,D;\Theta) \;=\; w_n\frac{\partial}{\partial t}\mathfrak{C}^{\mathrm{E}}_{t_{n-1}}(L;t_n,H_i)+w^{\mathrm{bin}}\frac{\partial}{\partial t}\mathfrak{C}^{\mathrm{bin}}_{t_{n-1}}(L;t_n,L).$$

Note here that only the thetas at $t_{n-1}$ are matched in order to keep the number of hedging instruments as small as possible. The case of UOPB is similarly handled. Although not reported, it is observed that their mismatch values are significantly reduced. The theta $\theta_t(x,d;\Theta)$ for the Parisian options under the jump-diffusion model (1) is computed and reported in the appendix.

Lastly, we would like to mention another interesting variant of barrier options, known as *Parasian options*. It differs from Parisian options in that the excursion time for the trigger to be activated accumulates whenever the asset price stays below the barrier. Its valuation is discussed in Chesney et al. [1997] under the name of cumulative Parisian options. The quasi-static hedging strategy for Parasian options can be designed in a similar manner. That is, we first decompose the option into some contingent claims. Next, SHPs are constructed for each of those options. More specifically, we denote $\widetilde{\mathfrak{B}}^{\mathrm{d\cdot i}}_t(x,T_1;\Theta)$ with $x>L$ for the option that is the same as $\mathfrak{B}^{\mathrm{d\cdot i}}$ except that the payoff at $t^*$ is $\widetilde{\mathfrak{C}}_{t^*}(L,d;\Theta)$, the Parasian option value. Here, $t^*$ is the hitting time of the barrier $L$ and $d$ is the remaining window. Likewise, we define $\widetilde{\mathfrak{B}}^{\mathrm{u\cdot i}}_t(x,T_1;\Theta)$ with $x<L$ but in this case the payoff at $t^*$ is $\widetilde{\mathfrak{C}}_{t^*}(L,d-(t^*-t);\Theta)$.

The next proposition is the key identities for the quasi-static hedging of Parasian options. Its proof is similar to that of Proposition 1, and hence, not included here.

**Proposition 2** *Consider a Parasian down-and-in call $\widetilde{\mathfrak{C}}_t(x,d;\Theta)$ with $\Theta=\{T,L,K,D\}$. Then, the following relationships hold.*

1. *<u>case $x>L$</u>: for $0\le t<T$,*

$$\widetilde{\mathfrak{C}}_t(x,d;\Theta)=\widetilde{\mathfrak{B}}^{\mathrm{d\cdot i}}_t(x,T-d;\Theta);$$

2. *case $x < L$: for $0 \le t < T - d$,*

$$\widetilde{\mathfrak{C}}_t(x, d; \Theta) = \widetilde{\mathfrak{B}}_t^{\mathrm{u\cdot i}}(x, t + d; \Theta) + \widetilde{\mathfrak{B}}_t^{\mathrm{u\cdot o\cdot partial}}(x, t + d; \Theta).$$

# 5 Numerical results

## 5.1 Implementing quasi-static hedge

In our implementation of a quasi-static hedge, we focus on the case $S_0 > L$ without loss of generality. The following strictly increasing stopping times are considered:

$$t^*_{2l+1} = \inf\{t > t^*_{2l} + \varepsilon | S_t < L\}, \qquad t^*_{2l+2} = \inf\{t > t^*_{2l+1} + \varepsilon | S_t > L\}$$

for $l = 0, 1, \ldots$ and $t^*_0 = 0$. Here $\varepsilon$ is introduced in order to control the hedging frequency but a small $\varepsilon$ close to zero works well in the numerical experiments. We denote the hedging error at time $t$ by $\mathsf{HE}_t$.

(i) At time 0, construct $\pi_0\left(S_0; \mathfrak{B}^{\mathrm{d\cdot i}}\right)$ and set $l = 0$, $\mathsf{HE}_0 = 0$;

(ii) At the next stopping time $t^*_{2l+1}$, do the followings;

(a) Suppose $t^*_{2l+1} < T - D$. Unwind the portfolio and compute

$$\mathsf{HE}_{t^*_{2l+1}} = \mathsf{HE}_{t^*_{2l}} e^{r(t^*_{2l+1} - t^*_{2l})} + \mathfrak{C}_{t^*_{2l+1}}(S_{t^*_{2l+1}}, D; \Theta) - \pi_{t^*_{2l+1}}\left(S_{t^*_{2l+1}}; \mathfrak{B}^{\mathrm{d\cdot i}}\right).$$

Construct an SHP(DIP+UOPB) with value $\pi_{t^*_{2l+1}}\left(S_{t^*_{2l+1}}; \mathfrak{B}^{\mathrm{u\cdot i}}\right) + \pi_{t^*_{2l+1}}\left(S_{t^*_{2l+1}}; \mathfrak{B}^{\mathrm{u\cdot o\cdot partial}}\right)$.

(b) Suppose $t^*_{2l+1} \ge T - D$. The Parisian option as well as the portfolio of put options expire worthless and the final hedging error is given by $\mathsf{HE}_{t^*_{2l}} e^{r(T - D - t^*_{2l})}$.

(iii) At the next stopping time $t^*_{2l+2}$ with the remaining window $d$, do the followings;

(a) Suppose $t^*_{2l+2} < \min\{t^*_{2l+1} + d, T - D\}$. Unwind the portfolio and compute

$$\begin{aligned}\mathsf{HE}_{t^*_{2l+2}} \;=\; & \mathsf{HE}_{t^*_{2l+1}} e^{r(t^*_{2l+2} - t^*_{2l+1})} + \mathfrak{C}_{t^*_{2l+2}}(S_{t^*_{2l+2}}, D; \Theta) \\ & - \pi_{t^*_{2l+2}}\left(S_{t^*_{2l+2}}; \mathfrak{B}^{\mathrm{u\cdot i}}\right) - \pi_{t^*_{2l+2}}\left(S_{t^*_{2l+2}}; \mathfrak{B}^{\mathrm{u\cdot o\cdot partial}}\right).\end{aligned}$$

Construct an SHP(DIB) with value $\pi_{t^*_{2l+2}}\left(S_{t^*_{2l+2}}; \mathfrak{B}^{\mathrm{d\cdot i}}\right)$.

(b) Suppose $t^*_{2l+2} < t^*_{2l+1} + d$ but $t^*_{2l+2} \ge T - D$. The Parisian option expires worthless at $t^*_{2l+2}$. Unwind the portfolio and the final hedging error is given by

$$\mathsf{HE}_{t^*_{2l+2}} = \mathsf{HE}_{t^*_{2l+1}} e^{r(t^*_{2l+2} - t^*_{2l+1})} - \pi_{t^*_{2l+2}}\left(S_{t^*_{2l+2}}; \mathfrak{B}^{\mathrm{u\cdot o\cdot partial}}\right).$$

(c) Suppose $t^*_{2l+2} \geq t^*_{2l+1} + d$. The Parisian option as well as the portfolio become vanilla calls with maturity $T$. The final hedging error is $\mathsf{HE}_{t^*_{2l+1}} e^{rd}$.

(iv) Increase $l$ by 1 and go back to Step (ii).

In the numerical experiments, the parameter values are the same as in Table 1. Each sample path of the stock price is generated for 4800 time steps with a constant step size. For each sample path, the quasi-static hedge is conducted as stated above. The final hedging errors are normalized by the option price $\mathfrak{C}_0(S_0, D; \Theta)$ or simply $\mathfrak{C}_0$ and then we denote their magnitudes as $\mathsf{HE}$ like in dynamic hedging. The strike prices of the vanilla options are the barrier level, i.e. $H_i = L$, $i = 1, \cdots, n$. Additionally, the time step $(t_i - t_{i-1})$ is fixed to 1/12, 1/24, 1/48 during the hedging period.

As for dynamic delta hedging, a hedging portfolio is re-balanced at discrete time steps $t_i = i\delta t$ for $i = 1, 2, \ldots, n$ with $\delta t = T/n$, as follows (see Coleman et al. [2003]):

(i) Let us denote the portfolio value, the number of shares of the underlying stock, and the deposit at a bank account by $\pi_t$, $\Delta_t$, and $B_t$, respectively. The initial portfolio consists of a long Parisian call $\mathfrak{C}_0$ and short $\Delta_0$ shares. By making a deposit $B_0 = \Delta_0 S_0 - \mathfrak{C}_0$, the initial portfolio value $\pi_0$ becomes zero.

(ii) At each time step $t_i$, the hedging portfolio is updated according to the realized option and stock prices. We note that its value is given by

$$\pi_{t_i} = \mathfrak{C}_{t_i} - \Delta_{t_{i-1}} S_{t_i} - B_{t_{i-1}} e^{r\delta t} = \mathfrak{C}_{t_i} - \Delta_{t_i} S_{t_i} - B_{t_i}$$

where $B_{t_i}$ is set to make the equation hold.

(iii) Hedging operations are performed until the option is expired or knocked-in, say time $t^*$. We record the final hedging error $\mathsf{HE} := |\pi_{t^*}|/\mathfrak{C}_0$ normalized by the option price.

## 5.2 Hedging performance under the jump-diffusion dynamics

We first investigate the hedging performance of the proposed static hedging method by considering four different sets of jump parameters; we consider $\lambda \in \{3, 5\}$ and the jump rates $\eta_i \in \{25, 50\}$. A total of 200 paths are used for each experiment. Tables 5 and 6 show the numerical results for the static hedging and dynamic hedging, respectively, in terms of the mean, VaR and ES of the hedging error $\mathsf{HE}$.

From the results, it is obvious that static hedging yields better results than dynamic hedging does. In particular, an $\mathsf{SHP}$ even with monthly dispersed vanilla options is superior to dynamic hedging with 240 time steps which roughly corresponds to daily re-balancing. Such performance differences can be understood as

Table 5: Mean, value-at-risk, and expected shortfall of simulated HE with parameter values in Table 1 and sample size 200.

| $\lambda$ | $\eta_1$,$\eta_2$ | interval | mean | $\mathrm{VaR}_{0.1}(\%)$ | $\mathrm{ES}_{0.1}(\%)$ | $\mathrm{VaR}_{0.05}(\%)$ | $\mathrm{ES}_{0.05}(\%)$ |
|---|---|---|---|---|---|---|---|
| 3 | 50 | monthly(1/12) | 7.46 | 15.75 | 31.91 | 21.81 | 46.45 |
| | | biweekly(1/24) | 4.80 | 8.06 | 31.30 | 20.13 | 49.43 |
| | | weekly(1/48) | 4.35 | 8.71 | 33.33 | 24.45 | 51.60 |
| 3 | 25 | monthly(1/12) | 11.06 | 20.27 | 67.91 | 33.21 | 112.58 |
| | | biweekly(1/24) | 8.75 | 10.41 | 67.84 | 33.96 | 119.23 |
| | | weekly(1/48) | 8.46 | 11.08 | 70.13 | 35.64 | 122.35 |
| 7 | 50 | monthly(1/12) | 10.11 | 25.39 | 59.30 | 45.60 | 86.79 |
| | | biweekly(1/24) | 5.78 | 11.08 | 41.12 | 23.60 | 66.00 |
| | | weekly(1/48) | 4.29 | 6.27 | 35.73 | 15.39 | 60.84 |
| 7 | 25 | monthly(1/12) | 11.95 | 35.99 | 64.80 | 58.81 | 83.95 |
| | | biweekly(1/24) | 7.77 | 24.18 | 49.09 | 40.13 | 65.10 |
| | | weekly(1/48) | 6.73 | 23.85 | 46.36 | 40.50 | 61.70 |

follows. First, while all the jumps that occur in a hedging period have adverse effects on the performance of the dynamic hedging, static hedging is affected only by overshoots when the asset price crosses the barrier. Second, a dynamic hedging portfolio is exposed to severe gamma and theta risks if an excursion below the barrier is in progress as described in Section 3.

As our last observation, we note that the performance of an SHP does not improve when the calendar-spread is smaller. For instance, the "weekly" SHP has the best results in terms of the mean of HE. However, the "biweekly" SHP outperforms the other two in terms of VaR and ES. The reason is because the proposed static hedge does not converge to the true price of the corresponding Parisian option due to the presence of the jumps. To overcome such negative effects of the jumps (overshoot, non-convergence), one could consider matching the values of an SHP and the target option beyond the barrier level, by adding more vanilla options.

We indeed tried this idea by having one additional vanilla option with a strike other than $L$. In the case of UIB, for instance, we add $\mathfrak{C}_t^{\mathrm{E}}(x; t_n, H)$ to (7). The coefficient for this new option is determined by adding the following equation to (8):

$$\mathfrak{C}_{t_{n-1}}(H, D; \Theta) \;=\; \pi^{(n)}_{t_{n-1}}\left(H; \mathfrak{B}^{\mathrm{u\cdot i}}\right).$$

In our implementation, we set $H$ equal to the mean of the jump sizes. Static hedges of other exotic options are constructed in a similar fashion. Although not reported to economize on space, the inclusion of additional vanilla options does not improve the hedging performance. Hence, one should be careful in treating overshoots or undershoots caused by jumps. Indeed, adding vanilla options with inappropriate strikes

Table 6: Mean, value-at-risk, and expected shortfall of simulated HE with parameter values in Table 1 and sample size 200.

| $\lambda$ | $\eta_1$,$\eta_2$ | # of time steps | mean | $\mathrm{VaR}_{0.1}$(%) | $\mathrm{ES}_{0.1}$(%) | $\mathrm{VaR}_{0.05}$(%) | $\mathrm{ES}_{0.05}$(%) |
|---|---|---|---|---|---|---|---|
| 3 | 50 | 120 | 51.84 | 139.88 | 232.79 | 207.45 | 299.70 |
| | | 240 | 40.71 | 108.19 | 200.18 | 155.79 | 267.31 |
| 3 | 25 | 120 | 51.90 | 150.71 | 227.35 | 209.88 | 296.06 |
| | | 240 | 46.05 | 133.91 | 211.96 | 172.92 | 287.55 |
| 7 | 50 | 120 | 46.52 | 101.93 | 206.42 | 179.26 | 278.77 |
| | | 240 | 40.90 | 93.80 | 199.70 | 138.84 | 285.03 |
| 7 | 25 | 120 | 52.82 | 139.26 | 206.84 | 179.00 | 262.75 |
| | | 240 | 46.63 | 123.28 | 197.97 | 170.97 | 261.64 |

may deteriorate the matching quality of the value functions of a target option and a hedging portfolio. This phenomenon is consistent with the results in Nalholm and Poulsen [2006] where the authors find that the performance does not improve when hedging the jump component. We leave this interesting topic to be fully explored in the future.

### 5.3 Special case: the Black-Scholes dynamics

Setting $\lambda = 0$ reduces (1) to the classical Black-Scholes model. Previously in Section 3, we reported the dynamic hedging results of Parisian options under the Black-Scholes dynamics. In this section, we focus on this special case and compare the hedging performance of dynamic delta hedging with static hedging. In particular, we consider different static hedging methods and compare their performances:

1. calendar-spread approach;
2. theta-matching approach in Section 4.4.
3. unified approach explained in Section 4.2;

On the other hand, recall that the construction in Section 4.3 does not prevent us from choosing the vanilla option strikes $H_i$'s other than $L$ as long as the expiration boundaries of the vanilla options and the target option are matched. For instance, any European put option whose strike is below the barrier can be used to construct an SHP(DIB). Such flexibility is quite beneficial from a practical standpoint because one can avoid using illiquid vanilla options.

Another practicality is achieved by choosing a suitable set of strikes which makes the corresponding hedging portfolio more akin to the target. As one example, we use vanilla options with the same strike

$H = H_i \leq L$ for all $i$ and we optimally choose $H$ in order to match the thetas of the target option and the hedging portfolio at time 0. More specifically, assume $H \in \mathfrak{X} = \{k \in \mathbb{N} | 85 \leq k \leq 95\}$. Let us denote the $n$-point SHP(DIB) by $\pi_t^{(n)}\left(x; \mathfrak{B}^{\mathrm{d\cdot i}}, H\right)$ to emphasize that the vanilla strikes are $H$. Then, the problem of optimally constructing an $n$-point SHP with $H^*$ can be described as follows:

$$\min_{H \in \mathfrak{X}, H \leq L} \quad \left| \frac{\partial}{\partial t} \pi_0^{(n)} \left( L; \mathfrak{B}^{\mathrm{d\cdot i}}, H \right) - \theta_0(L, D; \Theta) \right|$$

where $\pi^{(n)}$ is constructed by (5) and $w_i$'s solve (6) with $H_i = H$ for all $i$.

We, therefore, implement this idea in our comparison:

4. theta-matching approach with optimal $H^*$;

5. unified approach with optimal $H^*$.

These approaches are quit promising as one can see from the differences in the value functions of DIB and its SHP in Figure 9.[10]

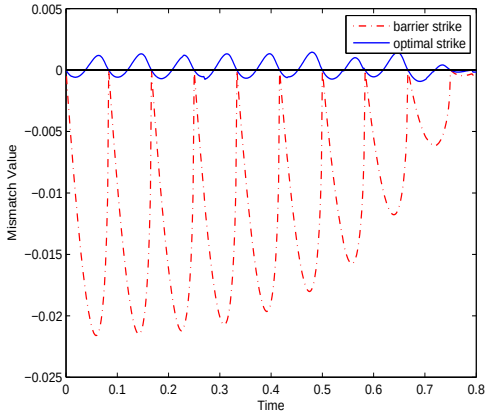


Figure 9: Mismatch values between the value functions of the SHP(DIB) with strike $L$ and the SHP(DIB) with strike $H^*$ for $s \in [0, T - D]$; $D = 0.2$, monthly interval and other parameter values are as in Table 1 .

Table 7 summarizes the numerical outcomes. We note that hedging performances are improved significantly compared to those of dynamic hedging in Table 2. In particular, "weekly" horizontal approach performs better than the dynamic hedging with 2400 time steps (this means approximately 10 daily rebalancing). This is true for the calendar-spread approach as well. When the theta-matching condition or the unified approach is incorporated, even the "monthly" case shows improved performances over the delta hedging with 2400 time steps. Furthermore, an SHP can do better with the extra cost of computing optimal strike $H^*$. As shown in the last two rows of Table 7, the SHPs with monthly dispersed options are comparable to the "weekly" SHPs.

Table 7: Mean, value-at-risk, and expected shortfall of simulated HE of quasi-static hedging with parameter values in Table 1 and sample size 1000.

| strike | method | interval | mean | $\mathrm{VaR}_{0.1}(\%)$ | $\mathrm{ES}_{0.1}(\%)$ | $\mathrm{VaR}_{0.05}(\%)$ | $\mathrm{ES}_{0.05}(\%)$ |
|---|---|---|---|---|---|---|---|
| $L$ | calendar-spread | monthly(1/12) | 28.73 | 78.12 | 141.50 | 103.99 | 193.40 |
| | | biweekly(1/24) | 14.44 | 25.74 | 92.10 | 47.53 | 150.40 |
| | | weekly(1/48) | 5.68 | 8.09 | 37.41 | 16.48 | 64.13 |
| $L$ | theta-matching | monthly(1/12) | 7.48 | 19.30 | 35.16 | 25.65 | 48.33 |
| | | biweekly(1/24) | 5.45 | 13.65 | 29.55 | 19.91 | 43.06 |
| | | weekly(1/48) | 4.52 | 10.86 | 26.50 | 16.20 | 39.67 |
| $L$ | unified | monthly(1/12) | 10.51 | 23.70 | 37.39 | 28.77 | 48.63 |
| | | biweekly(1/24) | 5.22 | 9.72 | 25.95 | 17.54 | 40.87 |
| | | weekly(1/48) | 4.12 | 7.11 | 28.57 | 13.54 | 46.24 |
| opt | theta-matching | monthly(1/12) | 4.47 | 10.28 | 26.79 | 16.78 | 40.72 |
| opt | unified | monthly(1/12) | 4.55 | 10.90 | 30.46 | 20.15 | 46.85 |

# 6 Conclusion

In this paper, we examined Parisian options from a risk management point of view. First, we investigated the performance of dynamic delta hedging under the Black-Scholes dynamics. From the experiments, it was observed that dynamic hedging might result in huge hedging errors. The path-by-path investigation then showed that such phenomenon arises due to severe gamma and theta values especially when the Brownian excursion is in progress. The problem becomes aggravated if we include jumps in the asset dynamics. This is in contrast with the well-known cushion effect of Parisian options, and thus poses a great challenge for a risk manager.

In order to resolve this problem, we proposed a quasi-static hedging strategy which can actually be extended to more general asset dynamics than the jump-diffusion model of double-exponential type. The key step in the hedging procedure is to decompose the value of a Parisian option into those of other contingent claims. Each of these claims is an exotic version of barrier options and we were able to apply the unified approach in constructing static hedging portfolios. In particular, the hedging portfolios consisted of vanilla calls or puts together with binary options. In the numerical experiments, the suggested hedging method yielded superior results compared to dynamic delta hedging under the jump-diffusion model. Especially for the Black-Scholes case with a zero jump rate, we compared variants of the proposed hedging strategy. It was noticed that the theta-matching method was comparable to the unified method, and these two performed much better than the calendar-spread approach. Furthermore, static hedging portfolios with suitably chosen option strikes were shown to have greatly improved performance.

There are still relevant and interesting questions to explore in the future. One can investigate whether the proposed idea is applicable to variations of Parisian options. Moreover, a more thorough empirical study on hedging performance can be considered as well, including market frictions such as transaction costs. More importantly, it would be quite interesting to see how one can construct larger but better static hedging portfolios for Parisian options in the presence of asset price jumps.

## Notes

[1]In this paper, we mainly deal with delta, gamma (respectively the 1st and 2nd order sensitivities with respect to the underlying stock price) and theta (the sensitivity with respect to time).

[2]Although the approach of Bernard et al. [2005] can be applied to more general cases, the presentation itself was incomplete because it was restricted to the case where the asset price is above the barrier for a down-and-in Parisian option.

[3]The random variable $H_{L,t}$ depends on other parameters such as $D$. However, we use $H_{L,t}$ for notational simplicity as done in Schröder [2003].

[4]Since Albrecher et al. [2012] deal with up-and-in calls only, we also derive the formula for down-and-in calls for the reader's convenience.

[5]Throughout this paper, we do not specify risk premia for the model parameters. This is because our focus is on testing hedging performances for simulated asset scenarios. Inclusion of risk premia would not alter our conclusions. See Carr and Picron [1999] or Chung et al. [2013].

[6]Delta hedging for a Parisian call is performed until the option is expired or knocked-in as done in Chung and Shih [2009], Chung et al. [2013].

[7]In this paper, we assume that fractions of shares are tradable.

[8]The formulas for European call and put options with the Laplace transform are given in the appendix, or see Kou [2002] for other formulas expressed by the Hh functions.

[9]If the asset price dynamics does not contain a jump component, $S_{t^*} = L$. Otherwise, $S_{t^*}$ may not be $L$ due to an overshoot.

[10]The optimal strike $H^*$ for UIB and UOPB can be obtained in a similar fashion except that the theta-matching condition at $t_{n-1}$ also needs to be added to the set of constraints. However, the strike of the binary option is always $L$ because of its particular role in the theta-matching portfolios. The same strike assumption $H = H_i$ for all $i$ can be relaxed. By considering heterogeneous strikes, value matching together with multiple theta-matching can be utilized to further reduce the mismatch values. Each optimal strike $H_i^*$ is calculated by backward recursion.


### Acknowledgement

The authors are grateful for the helpful comments of an anonymous referee in improving the presentation of the manuscript. The authors also thank Prof. A. Dassios for sharing his recent paper on Parisian options. The research of K. Kim was supported by the Basic Science Research Program through the National Research Foundation of Korea funded by the Ministry of Education (NRF-2014R1A1A2054868).

## References


H. Albrecher, D. Kortschak, and X. Zhou. Pricing of Parisian options for a jump-diffusion model with two-sided jumps. *Applied Mathematical Finance*, 19:97–129, 2012.

J. H. M. Anderluh and J. A. M. van der Weide. Double-sided Parisian option pricing. *Finance and Stochastics*, 13:205–238, 2009.

M. Avellaneda and L. Wu. Pricing Parisian-style options with a lattice method. *International Journal of Theoretical and Applied Finance*, 2:1–16, 1999.

Bank for International Settlements. OTC derivatives statistics at end-December 2014. 2015. Basel: Bank for International Settlements.

C. Bernard, O. Le Courtois, and F. Quittard-Pinon. A new procedure for pricing Parisian options. *Journal of Derivatives*, 12:45–53, 2005.

J. Bowie and P. Carr. Static simplicity. *Risk*, 7:44–50, 1994.

P. Carr and A. Chou. Breaking barriers. *Risk*, 10:139–145, 1997.

P. Carr and J.-F. Picron. Static hedging of timing risk. *Journal of Derivatives*, 6:57–70, 1999.

P. Carr, K. Ellis, and V. Gupta. Static hedging of exotic options. *Journal of Finance*, 53:1165–1190, 1998.

A. Chen and M. Suchanecki. Parisian exchange options. *Quantitative Finance*, 11:1207–1220, 2011.

M. Chesney and L. Gauthier. American Parisian options. *Finance and Stochastics*, 10:475–506, 2006.

M. Chesney, M. Jeanblanc-Picqué, and M. Yor. Brownian excursions and Parisian barrier options. *Advances in Applied Probability*, 29:165–184, 1997.

S. Chung and P. Shih. Static hedging and pricing American options. *Journal of Banking and Finance*, 33: 2140–2149, 2009.

S. Chung, P. Shih, and W. Tsai. A modified static hedging method for continuous barrier options. *Journal of Futures Markets*, 30:1150–1166, 2010.

S. Chung, P. Shih, and W. Tsai. Static hedging and pricing American knock-in put options. *Journal of Banking and Finance*, 37:191–205, 2013.

T. F. Coleman, K. Yohan, L. Yuying, and V. Arun. Dynamic hedging with a deterministic local volatility function model. 2003. Working Paper.

I. Czarna and Z. Palmowski. Ruin probability with Parisian delay for a spectrally negative Lévy risk process. *Journal of Applied Probability*, 48:984–1002, 2011.

A. Dassios and J. W. Lim. Parisian option pricing: A recursive solution for the density of the Parisian stopping time. *SIAM Jounral on Financial Mathmatics*, 4:599–615, 2013.

A. Dassios and J. W. Lim. An analytical solution for the two-sided Parisian stopping time, its asymptotics and the pricing of Parisian options. *Mathematical Finance*, 2014. Forthcoming.

A. Dassios and S. Wu. Double-barrier Parisian options. *Journal of Applied Probability*, 48:1–20, 2011.

E. Derman, D. Ergener, and I. Kani. Static options replication. *Journal of Derivatives*, 2:78–95, 1995.

E. Gobet and E. Temam. Discrete time hedging errors for options with irregular payoffs. *Finance and Stochastics*, 5:357–367, 2001.

R. J. Haber, P. J. Schönbucher, and P. Wilmott. Pricing Parisian options. *Journal of Derivatives*, 6:71–79, 1999.

S. G. Kou. A jump-diffusion model for option pricing. *Management Science*, 48:1086–1101, 2002.

C. Labart and J. Lelong. Pricing Parisian options using Laplace transforms. *Bankers Markets and Investors*, 99:1–24, 2009.

A. C. H. Lei. Price and volume effects of exchange-traded barrier options: Evidence from callable bull/bear contracts. *Journal of Futures Markets*, 2014. Forthcoming.

R. Loeffen, I. Czarna, and Z. Palmowski. Parisian ruin probability for spectrally negative Lévy processes. *Bernoulli*, 19:599–609, 2013.

M. Nalholm and R. Poulsen. Static hedging of barrier options under gerneral asset dynamics: Unification and application. *Journal of Derivatives*, 13:46–60, 2006.

M. Schröder. Brownian excursions and Parisian barrier options: A note. *Journal of Applied Probability*, 40: 855–864, 2003.

Supplementary material for
Risk Analysis and Hedging of Parisian Options under a Jump-diffusion Model

In this supplement, we record the necessary formulae to conduct dynamic hedging and static hedging as in the main body. For dynamic hedging, Parisian option prices and deltas under the jump-diffusion dynamics and the Black-Scholes model are reviewed. For static hedging, vanilla option prices and binary option prices in addition to Parisian option prices are given for the two models. Furthermore, Parisian option theta formulae are presented in order to implement the theta-matching method.

# A Parisian Down-and-in Call under a Jump-diffusion Dynamics

Albrecher et al. [2012] presented the valuation formula of Parisian up-and-in options under the dynamics (1). In this section, we describe the valuation procedure of Parisian down-and-in call options. The approach is the same as in Albrecher et al. [2012], nonetheless, we include it here for the reader's convenience and also for completeness.

First we set $X_t = \log S_t$ and $x = \log S_0$. Then, we can write the option price at time 0 by

$$\mathfrak{C}_0(S_0, D; \Theta) = e^{-rT}\mathsf{E}^x\left[\left(e^{X_T} - K\right)^+; H_{L,0} \leq T\right]$$

where $\mathsf{E}^x$ denotes the expectation with the initial condition $X_0 = x$. The presentation below is focused on the case of $L = 1$ and the case $d = D$; however, the general case of any $L$ and $d \leq D$ can be easily recovered as in Remarks 4.2 an 4.3 of Albrecher et al. [2012].

The Laplace transform of the call price is written as

$$\begin{aligned}\widehat{\mathfrak{C}}(\alpha) &= \int_0^\infty e^{-\alpha T}\mathfrak{C}_0(S_0, D; \Theta)dT \\ &= \int_{-\infty}^\infty (e^x - K)^+ \mathfrak{L}_{\alpha,D}(x, dy)\end{aligned}$$

where

$$\mathfrak{L}_{\alpha,D}(x, dy) = \frac{1}{\alpha}\mathsf{E}^x\left[e^{-re_\alpha}; H_{L,0} < e_\alpha, X_{e_\alpha} \in dy\right]$$

and $e_\alpha$ is the exponential random variable with rate $\alpha$. A careful analysis of this expectation $\mathfrak{L}_{\alpha,D}$ leads to the valuation formula in the original paper: for $x \geq 0$,

$$\begin{aligned}\widehat{\mathfrak{C}}(\alpha) &= \Gamma_1(r+\alpha, -x)\frac{B_1(\alpha, D)\tilde{A}_3(\alpha, D, K) + B_4(\alpha, D)\tilde{A}_2(\alpha, D, K)}{B_2(\alpha, D)B_4(\alpha, D) - B_1(\alpha, D)B_3(\alpha, D)} \\ &\quad + \Gamma_2(r+\alpha, -x)\frac{B_2(\alpha, D)\tilde{A}_3(\alpha, D, K) + B_3(\alpha, D)\tilde{A}_2(\alpha, D, K)}{B_2(\alpha, D)B_4(\alpha, D) - B_1(\alpha, D)B_3(\alpha, D)}\end{aligned}$$

and for $x < 0$,

$$\begin{aligned}\widehat{\mathfrak{C}}(\alpha) &= \tilde{A}_1(\alpha, D, x, K) \\ &\quad + \left(B_5(\alpha, D, x) + B_6(\alpha, D, x)\widehat{\Gamma}_1(r+\alpha, \eta_1)\right) \\ &\quad \times \frac{B_1(\alpha, D)\tilde{A}_3(\alpha, D, K) + B_4(\alpha, D)\tilde{A}_2(\alpha, D, K)}{B_2(\alpha, D)B_4(\alpha, D) - B_1(\alpha, D)B_3(\alpha, D)} \\ &\quad + B_6(\alpha, D, x)\widehat{\Gamma}_2(r+\alpha, \eta_1)\frac{B_2(\alpha, D)\tilde{A}_3(\alpha, D, K) + B_3(\alpha, D)\tilde{A}_2(\alpha, D, K)}{B_2(\alpha, D)B_4(\alpha, D) - B_1(\alpha, D)B_3(\alpha, D)}.\end{aligned}$$

We note that these formulae are almost the same as in p.111 of Albrecher et al. [2012]; however, the functions $\tilde{A}_i$'s, $B_i$'s, and $\Gamma_i$'s (and their transforms) are different.

The valuation consists of two steps. First, we compute the relevant functions in the formulae above by inverting their Laplace transforms, and second, the Laplace inversion of $\widehat{\mathfrak{C}}(\alpha)$ yields the target option price.

## A.1 Auxiliary functions

**Gamma and Lambda functions.** As in p.100 of Albrecher et al. [2012], the four solutions of $t^{-1}\log \mathsf{E}\left[e^{\theta X_t}\right] = \alpha$ for $\alpha > 0$ are $\beta_1, \beta_2, -\beta_3$ and $-\beta_4$ such that

$$0 < \beta_1 < \eta_1 < \beta_2, \quad 0 < \beta_3 < \eta_2 < \beta_4.$$

With $\nu_b^- = \inf\{t \geq 0 | X_t < b\}$ and $b < 0$, we have

$$\begin{aligned}\Gamma_1(\alpha, b) &= \mathsf{E}^0\left[e^{-\alpha\nu_b^-}; X_{\nu_b^-} = b\right] = \frac{\eta_2 - \beta_3}{\beta_4 - \beta_3}e^{b\beta_3} - \frac{\eta_2 - \beta_4}{\beta_4 - \beta_3}e^{b\beta_4}, \\ \Gamma_2(\alpha, b) &= \mathsf{E}^0\left[e^{-\alpha\nu_b^-}; X_{\nu_b^-} < b\right] = \frac{(\eta_2 - \beta_3)(\eta_2 - \beta_4)}{\eta_2(\beta_4 - \beta_3)}\left(e^{b\beta_4} - e^{b\beta_3}\right).\end{aligned}$$

Their Laplace transforms are given as

$$\begin{aligned}\widehat{\Gamma}_1(\alpha, s) &= \int_0^\infty \mathrm{d}use^{-su}\Gamma_1(\alpha, -u) = \frac{s}{\beta_4 - \beta_3}\left(\frac{\eta_2 - \beta_3}{s + \beta_3} - \frac{\eta_2 - \beta_4}{s + \beta_4}\right), \\ \widehat{\Gamma}_2(\alpha, s) &= \int_0^\infty \mathrm{d}use^{-su}\Gamma_2(\alpha, -u) = \frac{(\eta_2 - \beta_3)(\eta_2 - \beta_4)}{\eta_2(\beta_4 - \beta_3)}\left(\frac{s}{s + \beta_4} - \frac{s}{s + \beta_3}\right).\end{aligned}$$

On the other hand, the same functions and their Laplace transforms for the process $-X_t$ turn out to be useful. For instance, $\Gamma_1^*(\alpha, b)$ for $b < 0$ is defined as $\Gamma_1(\alpha, b)$ but $X_t$ replaced with $-X_t$. Then, for $b < 0$, we have

$$\begin{aligned}\Gamma_1^*(\alpha, b) &= \frac{\eta_1 - \beta_1}{\beta_2 - \beta_1}e^{b\beta_1} - \frac{\eta_1 - \beta_2}{\beta_2 - \beta_1}e^{b\beta_2}, \\ \Gamma_2^*(\alpha, b) &= \frac{(\eta_1 - \beta_1)(\eta_1 - \beta_2)}{\eta_1(\beta_2 - \beta_1)}\left(e^{b\beta_2} - e^{b\beta_1}\right), \\ \widehat{\Gamma}_1^*(\alpha, s) &= \frac{s}{\beta_2 - \beta_1}\left(\frac{\eta_1 - \beta_1}{s + \beta_1} - \frac{\eta_1 - \beta_2}{s + \beta_2}\right),\end{aligned}$$

$$\widehat{\Gamma}_2^*(\alpha, s) = \frac{(\eta_1 - \beta_1)(\eta_1 - \beta_2)}{\eta_1(\beta_2 - \beta_1)} \left( \frac{s}{s + \beta_2} - \frac{s}{s + \beta_1} \right).$$

For a later use in the computation of greeks, we introduce new functions $\Gamma_3$, $\Gamma_4$, $\Gamma_3^*$ and $\Gamma_4^*$ that are defined as

$$\Gamma_3(\alpha, b) = \frac{\partial \Gamma_1(\alpha, b)}{\partial b}, \quad \Gamma_3^*(\alpha, b) = \frac{\partial \Gamma_1^*(\alpha, b)}{\partial b}, \quad \Gamma_4(\alpha, b) = \frac{\partial \Gamma_2(\alpha, b)}{\partial b}, \quad \Gamma_4^*(\alpha, b) = \frac{\partial \Gamma_2^*(\alpha, b)}{\partial b}.$$

The following functions are also needed:

$$\begin{aligned}
\Lambda_1(\alpha) &= -\lim_{\epsilon \to 0+} \frac{\Gamma_1(\alpha, -\epsilon) - 1}{\epsilon} = \beta_3 + \beta_4 - \eta_2, \\
\Lambda_2(\alpha) &= \lim_{\epsilon \to 0+} \frac{\Gamma_2(\alpha, -\epsilon) - 0}{\epsilon} = -\frac{(\eta_2 - \beta_3)(\eta_2 - \beta_4)}{\eta_2} \\
\Lambda_1^*(\alpha) &= \lim_{\epsilon \to 0+} \frac{1 - \Gamma_1^*(\alpha, -\epsilon)}{\epsilon} = \beta_1 + \beta_2 - \eta_1 \\
\Lambda_2^*(\alpha) &= \lim_{\epsilon \to 0+} \frac{\Gamma_2^*(\alpha, -\epsilon)}{\epsilon} = -\frac{(\eta_1 - \beta_1)(\eta_1 - \beta_2)}{\eta_1}.
\end{aligned}$$

**Special Integrals.** The next integrals are given in p.117 of Albrecher et al. [2012]. Hence their explicit expressions are omitted.

$$\begin{aligned}
J_1(\alpha, \beta, k) &= \int_0^\infty \mathrm{d}y \alpha e^{-\beta y} (e^y - k)^+, \\
J_2(\alpha, \beta, k) &= \int_{-\infty}^0 \mathrm{d}y \alpha e^{\beta y} (e^y - k)^+, \\
J_3(\alpha, \beta, x, k) &= \int_x^\infty \mathrm{d}y \alpha e^{-\beta(y-x)} (e^y - k)^+, \\
J_4(\alpha, \beta, x, k) &= \int_{-\infty}^x \mathrm{d}y \alpha e^{\beta(y-x)} (e^y - k)^+.
\end{aligned}$$

There are additional special integrals as given in the original paper. Since we are dealing with the case $K > L$, we consider the case $k > 1$ and this simplifies the expressions:

$$\begin{aligned}
J_5(\eta, \alpha, \beta, k) &= \int_{-\infty}^\infty \mathrm{d}y \int_0^y \mathrm{d}x \alpha \eta e^{-\eta x} e^{-\beta(y-x)} (e^y - k)^+ \\
&= \alpha \left\{ \frac{e^{-(\eta-1)\log k}}{\eta - 1} - k \frac{e^{-\eta \log k}}{\eta} - \frac{e^{-(\beta-1)\log k}}{\beta - 1} + k \frac{e^{-\beta \log k}}{\beta} \right\} \frac{\eta}{\beta - \eta}, \\
J_6(\eta, \alpha, \beta, k) &= \int_{-\infty}^\infty \mathrm{d}y \int_y^\infty \mathrm{d}x \alpha \eta e^{-\eta x} e^{\beta(y-x)} (e^y - k)^+ = \frac{\alpha \eta}{\eta + \beta} \left( \frac{e^{-\log k(\eta-1)}}{\eta - 1} - \frac{k}{\eta} e^{-\eta \log k} \right), \\
J_7(\eta, \alpha, \beta, k) &= \int_{-\infty}^\infty \mathrm{d}y \int_0^\infty \mathrm{d}x \alpha \eta e^{-\eta x} e^{-\beta(y+x)} (e^y - k)^+ = \frac{\alpha \eta}{\eta + \beta} \frac{k^{1-\beta}}{(\beta - 1)\beta}.
\end{aligned}$$

## A.2 Laplace transforms of $\tilde{A}_i$'s and $B_i$'s

**Laplace transforms of $B_i$'s.** For each fixed $\alpha$, the transforms of $B_i$'s are computed with respect to the parameter $D$. Then straightforward computations yield

$$\begin{aligned}
\beta\widehat{B}_1(\alpha,\beta) &= \beta\int_0^\infty \mathrm{d}De^{-\beta D}B_1(\alpha,D) = \Lambda_2(r+\alpha)+\widehat{\Gamma}_2(r+\alpha,\eta_1)\Lambda_2^*(r+\alpha+\beta),\\
\beta\widehat{B}_2(\alpha,\beta) &= \beta\int_0^\infty \mathrm{d}De^{-\beta D}B_2(\alpha,D)\\
&= \Lambda_1(r+\alpha)+\Lambda_1^*(r+\alpha+\beta)-\widehat{\Gamma}_1(r+\alpha,\eta_1)\Lambda_2^*(r+\alpha+\beta),\\
\beta\widehat{B}_3(\alpha,\beta) &= \beta\int_0^\infty \mathrm{d}De^{-\beta D}B_3(\alpha,D) = \widehat{\Gamma}_1^*(r+\alpha+\beta,\eta_2)+\widehat{\Gamma}_2^*(r+\alpha+\beta,\eta_2)\widehat{\Gamma}_1(r+\alpha,\eta_1),\\
\beta\widehat{B}_4(\alpha,\beta) &= \beta\int_0^\infty \mathrm{d}De^{-\beta D}B_4(\alpha,D) = 1-\widehat{\Gamma}_2^*(r+\alpha+\beta,\eta_2)\widehat{\Gamma}_2(r+\alpha,\eta_1),\\
\beta\widehat{B}_5(\alpha,\beta,x) &= \beta\int_0^\infty \mathrm{d}De^{-\beta D}B_5(\alpha,D,x) = \Gamma_1^*(r+\alpha+\beta,x),\\
\beta\widehat{B}_6(\alpha,\beta,x) &= \beta\int_0^\infty \mathrm{d}De^{-\beta D}B_6(\alpha,D,x) = \Gamma_2^*(r+\alpha+\beta,x).
\end{aligned}$$

The functions $B_i$'s can be computed via Laplace inversion for each fixed $\alpha$ and $x$.

**Laplace transforms of $\tilde{A}_i$'s.** The expressions for these functions are quite intricate. We first introduce some constants:

$$\begin{aligned}
C_1^\alpha &= \frac{2}{\sigma^2}\frac{(\eta_1-\beta_1)(\eta_2+\beta_1)}{(\beta_2-\beta_1)(\beta_3+\beta_1)(\beta_4+\beta_1)},\\
C_2^\alpha &= \frac{2}{\sigma^2}\frac{(\eta_1-\beta_2)(\eta_2+\beta_2)}{(\beta_1-\beta_2)(\beta_3+\beta_2)(\beta_4+\beta_2)},\\
C_3^\alpha &= \frac{2}{\sigma^2}\frac{(\eta_1+\beta_3)(\eta_2-\beta_3)}{(\beta_1+\beta_3)(\beta_2+\beta_3)(\beta_4-\beta_3)},\\
C_4^\alpha &= \frac{2}{\sigma^2}\frac{(\eta_1+\beta_4)(\eta_2-\beta_4)}{(\beta_1+\beta_4)(\beta_2+\beta_4)(\beta_3-\beta_4)}.
\end{aligned}$$

Second, we present the Laplace transforms. Note that the transforms are computed with respect to the parameter $D$ for all other parameters fixed.

$$\begin{aligned}
\beta\widehat{\tilde{A}}_1(\alpha,\beta,x,K) &= J_3(C_1^{r+\alpha},\beta_1^{r+\alpha},x,K)+J_3(C_2^{r+\alpha},\beta_2^{r+\alpha},x,K)\\
&\quad -\Gamma_1^*(r+\alpha+\beta,x)\Big\{J_1(C_1^{r+\alpha},\beta_1^{r+\alpha},K)+J_1(C_2^{r+\alpha},\beta_2^{r+\alpha},K)\Big\}\\
&\quad -\Gamma_2^*(r+\alpha+\beta,x)\Big\{J_5(\eta_1,C_1^{r+\alpha},\beta_1^{r+\alpha},K)+J_5(\eta_1,C_2^{r+\alpha},\beta_2^{r+\alpha},K)\\
&\qquad +J_6(\eta_1,C_3^{r+\alpha},\beta_3^{r+\alpha},K)+J_6(\eta_1,C_4^{r+\alpha},\beta_4^{r+\alpha},K)\Big\},\\
\beta\widehat{\tilde{A}}_2(\alpha,\beta,K) &= J_1(-C_1^{r+\alpha}\beta_1^{r+\alpha},\beta_1^{r+\alpha},K)+J_1(-C_2^{r+\alpha}\beta_2^{r+\alpha},\beta_2^{r+\alpha},K)\\
&\quad +\Lambda_1^*(r+\alpha+\beta)\Big\{J_1(C_1^{r+\alpha},\beta_1^{r+\alpha},K)+J_1(C_2^{r+\alpha},\beta_2^{r+\alpha},K)\Big\}
\end{aligned}$$

$$
\begin{aligned}
&-\Lambda_2^*(r+\alpha+\beta)\Big\{J_5(\eta_1,C_1^{r+\alpha},\beta_1^{r+\alpha},K)+J_5(\eta_1,C_2^{r+\alpha},\beta_2^{r+\alpha},K)\\
&\qquad +J_6(\eta_1,C_3^{r+\alpha},\beta_3^{r+\alpha},K)+J_6(\eta_1,C_4^{r+\alpha},\beta_4^{r+\alpha},K)\Big\},\\
\beta\widehat{\tilde{A}}_3(\alpha,\beta,K) &= J_7(\eta_2,C_1^{r+\alpha},\beta_1^{r+\alpha},K)+J_7(\eta_2,C_2^{r+\alpha},\beta_2^{r+\alpha},K)\\
&\quad -\widehat{\Gamma}_1^*(r+\alpha+\beta,\eta_2)\Big\{J_1(C_1^{r+\alpha},\beta_1^{r+\alpha},K)+J_1(C_2^{r+\alpha},\beta_2^{r+\alpha},K)\Big\}\\
&\quad -\widehat{\Gamma}_2^*(r+\alpha+\beta,\eta_2)\Big\{J_5(\eta_1,C_1^{r+\alpha},\beta_1^{r+\alpha},K)+J_5(\eta_1,C_2^{r+\alpha},\beta_2^{r+\alpha},K)\\
&\qquad +J_6(\eta_1,C_3^{r+\alpha},\beta_3^{r+\alpha},K)+J_6(\eta_1,C_4^{r+\alpha},\beta_4^{r+\alpha},K)\Big\}.
\end{aligned}
$$

Note that $\beta_i^{r+\alpha}$'s are the solutions to the equation $t^{-1}\log\mathsf{E}\left[e^{\theta X_t}\right]=r+\alpha$ whereas $\beta_i$'s are the respective solutions with $r+\alpha$ replaced with $\alpha$ only.

### A.3 Parisian delta

We introduce new functions $B_7$ and $B_8$ for Parisian delta. More specifically, $B_7$ and $B_8$ are defined by the partial derivatives of $B_5$ and $B_6$ with respect to parameter $x$. These functions can be computed by inverting the following transforms for each fixed $\alpha, x$:

$$
\begin{aligned}
\beta\widehat{B}_7(\alpha,\beta,x) &= \Gamma_3^*(r+\alpha+\beta,x),\\
\beta\widehat{B}_8(\alpha,\beta,x) &= \Gamma_4^*(r+\alpha+\beta,x).
\end{aligned}
$$

These functions appear only when $x<0$.

On the other hand, as in the case of $B_i$'s, we define a new function $\tilde{A}_4$ which is the partial derivative of $\tilde{A}_1(\alpha,d,x,K)$ with respect to $x$. Its associated Laplace transform with respect to parameter $d$ is given as

$$
\begin{aligned}
\beta\widehat{\tilde{A}}_4(\alpha,\beta,x,K) &= J_3(C_1^{r+\alpha}\beta_1^{r+\alpha},\beta_1^{r+\alpha},x,K)+J_3(C_2^{r+\alpha}\beta_2^{r+\alpha},\beta_2^{r+\alpha},x,K)\\
&\quad -\Gamma_3^*(r+\alpha+\beta,x)\Big\{J_1(C_1^{r+\alpha},\beta_1^{r+\alpha},K)+J_1(C_2^{r+\alpha},\beta_2^{r+\alpha},K)\Big\}\\
&\quad -\Gamma_4^*(r+\alpha+\beta,x)\Big\{J_5(\eta_1,C_1^{r+\alpha},\beta_1^{r+\alpha},K)+J_5(\eta_1,C_2^{r+\alpha},\beta_2^{r+\alpha},K)\\
&\qquad +J_6(\eta_1,C_3^{r+\alpha},\beta_3^{r+\alpha},K)+J_6(\eta_1,C_4^{r+\alpha},\beta_4^{r+\alpha},K)\Big\}.
\end{aligned}
$$

Computation of delta is done in a straightforward fashion. First consider the case of $x\geq 0$. By changing the order of integration and differentiation, we obtain

$$
\widehat{\Delta}(\alpha)=\frac{\partial\widehat{\mathfrak{C}}(\alpha)}{\partial S_0}=-\frac{1}{S_0}\left[\Gamma_3\frac{B_1\tilde{A}_3+B_4\tilde{A}_2}{B_2B_4-B_1B_3}+\Gamma_4\frac{B_2\tilde{A}_3+B_3\tilde{A}_2}{B_2B_4-B_1B_3}\right]
$$

Similarly for $x<0$, we have

$$
\widehat{\Delta}(\alpha)=-\frac{1}{S_0}\left[\tilde{A}_4+\left(B_7+B_8\widehat{\Gamma}_1\right)\frac{B_1\tilde{A}_3+B_4\tilde{A}_2}{B_2B_4-B_1B_3}+B_8\widehat{\Gamma}_2\frac{B_2\tilde{A}_3+B_3\tilde{A}_2}{B_2B_4-B_1B_3}\right].
$$

Input parameters are the same as in the price formulae.

For general $L$, the option delta can be computed via the relationship

$$\Delta_t\Big(S_t, d; \{T, K, L, D\}\Big) = \Delta_t\left(\frac{S_t}{L}, d; \left\{T, \frac{K}{L}, 1, D\right\}\right).$$

This is contrasted with the case of the option price where we need to multiply $L$ to the option price with initial stock price $S_t/L$, strike $K/L$, and barrier 1.

### A.4 Parisian theta

Parisian theta with $S_0 \geq L$ can be easily obtained as follows :

$$\widehat{\theta}(\alpha) = -\alpha\widehat{\mathfrak{C}}(\alpha)$$

When the underlying asset is below the barrier, $S_0 < L$, we should additionally consider the sensitivity of the option price with respect to the remaining window, $\partial\mathfrak{C}/\partial d$. For this, we define new functions $\tilde{A}_5(\alpha, y, x, k)$, $B_9(\alpha, y, x)$ and $B_{10}(\alpha, y, x)$ by the partial derivatives of $\tilde{A}_1(\alpha, y, x, k)$, $B_5(\alpha, y, x)$ and $B_6(\alpha, y, x)$ with respect to $y$. Laplace transforms of these new functions with respect to $y$ can be obtained by

$$\begin{aligned}
\int_0^\infty e^{-\beta y}\tilde{A}_5(\alpha, y, x, k)\mathrm{d}y &= \beta\widehat{\tilde{A}}_1(\alpha, \beta, x, k) - \widehat{\mathfrak{C}}^{\mathrm{E}}(\alpha) \\
\int_0^\infty e^{-\beta y}B_9(\alpha, y, x)\mathrm{d}y &= \beta\widehat{B}_5(\alpha, \beta, x) \\
\int_0^\infty e^{-\beta y}B_{10}(\alpha, y, x)\mathrm{d}y &= \beta\widehat{B}_6(\alpha, \beta, x)
\end{aligned}$$

where $\widehat{\mathfrak{C}}^{\mathrm{E}}(\alpha)$ is the Laplace transform of the European call option which is given in Section C. Then, Parisian theta with $S_0 < L$ is given by

$$\widehat{\theta}(\alpha) = -\alpha\widehat{\mathfrak{C}}(\alpha) - \tilde{A}_5 - \Big(B_9 + B_{10}\widehat{\Gamma}_1\Big)\frac{B_1\tilde{A}_3 + B_4\tilde{A}_2}{B_2B_4 - B_1B_3} - B_{10}\widehat{\Gamma}_2\frac{B_2\tilde{A}_3 + B_3\tilde{A}_2}{B_2B_4 - B_1B_3}.$$

## B Parisian Down-and-in Call under the Black-Scholes Dynamics

### B.1 Pricing formulae

There have been several approaches to the Parisian option prices when the underlying asset follows a geometric Brownian motion. Our presentation is based on Schröder [2003] and Labart and Lelong [2009]. We

first consider the case $S_0 > L$. This makes $d = D$. Then, it is known that

$$\widehat{\mathfrak{C}}(\alpha) = \frac{\Psi(-\sqrt{2\mu D})e^{2b\sqrt{2\mu}}}{\Psi(\sqrt{2\mu D})\sqrt{2\mu}} \left(\frac{K}{S_0}\right)^{\frac{\varpi+\sigma-\sqrt{2\mu}}{\sigma}} \frac{S_0\sigma}{(\varpi-\sqrt{2\mu})(\varpi+\sigma-\sqrt{2\mu})};$$

where $b = \sigma^{-1}\log(L/S_0)$, $\varpi = r/\sigma - \sigma/2$, $\mu = r + \varpi^2/2 + \alpha$, and $\Psi(x) = 1 + x\sqrt{2\pi}e^{x^2/2}\Phi(x)$ with the cumulative distribution function $\Phi$ of the standard normal distribution.

Secondly, let us consider the case $S_0 \leq L$. We further assume that the excursion is in progress with the remaining window $d$. Then, it can be shown that

$$\widehat{\mathfrak{C}}(\alpha) = \widehat{\mathfrak{C}}^{\mathrm{E}}(\alpha) + e^{\varpi b}\left(\widehat{\mathfrak{C}}\,(\alpha; L, D) - \widehat{\mathfrak{C}}^{\mathrm{E}}(\alpha; L)\right)\int_0^d e^{-\mu u}\mu_b(\mathrm{d}u)$$

where $\mu_b(\mathrm{d}u) = |b|\left(2\pi u^3\right)^{-1/2} e^{-b^2/(2u)}\mathrm{d}u$ and $\widehat{\mathfrak{C}}^{\mathrm{E}}$ denotes the Laplace transform of a vanilla call with maturity $T$ and strike $K$. Here, $\widehat{\mathfrak{C}}(\alpha; L, D)$ has additional parameters in order to emphasize that the Laplace transform is evaluated at $S_0 = L$ and $d = D$. Similarly, $\widehat{\mathfrak{C}}^{\mathrm{E}}(\alpha; L)$ means the transform is computed at $S_0 = L$.

In Labart and Lelong [2009], a closed form formula for $\int_0^d e^{-\mu u}\mu_b(\mathrm{d}u)$ is given for the case $b > 0$:

$$\int_0^d e^{-\mu u}\mu_b(\mathrm{d}u) = e^{-b\sqrt{2\mu}}\Phi\left(\sqrt{2\mu d} - \frac{b}{\sqrt{d}}\right) + e^{b\sqrt{2\mu}}\Phi\left(-\sqrt{2\mu d} - \frac{b}{\sqrt{d}}\right). \tag{1}$$

Lastly, we record the Laplace transform of the European call price:

$$\widehat{\mathfrak{C}}^{\mathrm{E}}(\alpha) = \frac{1}{\sqrt{2\mu}}\left(\frac{K}{S_0}\right)^{\frac{\varpi+\sigma-\sqrt{2\mu}}{\sigma}} \frac{S_0\sigma}{(\varpi-\sqrt{2\mu})(\varpi+\sigma-\sqrt{2\mu})}.$$

## B.2 Parisian delta

The case of $S_0 \geq L$ (so that $d = D$) is handled in Bernard et al. [2005] by placing the derivative operator with respect to $S_0$ inside the integration. We simply note that

$$\begin{aligned}
\widehat{\Delta}(\alpha) &= -\frac{2\sqrt{2\mu}}{\sigma S_0}\cdot\frac{\Psi(-\sqrt{2\mu D})e^{2b\sqrt{2\mu}}}{\Psi(\sqrt{2\mu D})\sqrt{2\mu}}\left(\frac{K}{S_0}\right)^{\frac{\varpi+\sigma-\sqrt{2\mu}}{\sigma}}\frac{S_0\sigma}{(\varpi-\sqrt{2\mu})(\varpi+\sigma-\sqrt{2\mu})} \\
&\quad -\frac{\Psi(-\sqrt{2\mu D})e^{2b\sqrt{2\mu}}}{\Psi(\sqrt{2\mu D})\sqrt{2\mu}}\left(\frac{K}{S_0}\right)^{\frac{\varpi+\sigma-\sqrt{2\mu}}{\sigma}}\frac{1}{\varpi+\sigma-\sqrt{2\mu}} \\
&= -\frac{\Psi(-\sqrt{2\mu D})e^{2b\sqrt{2\mu}}}{\Psi(\sqrt{2\mu D})\sqrt{2\mu}}\left(\frac{K}{S_0}\right)^{\frac{\varpi+\sigma-\sqrt{2\mu}}{\sigma}}\frac{\varpi+\sqrt{2\mu}}{(\varpi-\sqrt{2\mu})(\varpi+\sigma-\sqrt{2\mu})}
\end{aligned}$$

and it is simplified to the expression in the statement.

Next, we focus on the case of $S_0 < L$ with the remaining window $d$. It turns out that the formula is given by

$$\widehat{\Delta}(\alpha) = \frac{e^{\varpi b}}{S_0\sigma}\left[\frac{1}{\sqrt{d}}\left\{e^{-b\sqrt{2\mu}}\phi\left(\sqrt{2\mu d} - \frac{b}{\sqrt{d}}\right) + e^{b\sqrt{2\mu}}\phi\left(-\sqrt{2\mu d} - \frac{b}{\sqrt{d}}\right)\right\}\right.$$

$$+(\sqrt{2\mu}-\varpi)e^{-b\sqrt{2\mu}}\Phi\left(\sqrt{2\mu d}-\frac{b}{\sqrt{d}}\right)-(\sqrt{2\mu}+\varpi)e^{b\sqrt{2\mu}}\Phi\left(-\sqrt{2\mu d}-\frac{b}{\sqrt{d}}\right)\Big]$$
$$\times\left(\widehat{\mathfrak{C}}\left(\alpha;L,D\right)-\widehat{\mathfrak{C}}^{\mathrm{E}}(\alpha;L)\right)+\widehat{\Delta}^{\mathrm{E}}(\alpha)$$

where $\phi$ is the probability density function of the standard normal and $\widehat{\Delta}^{\mathrm{E}}$ is the Laplace transform of the European call delta, which is obtained as follows via straightforward differentiation:

$$\widehat{\Delta}^{\mathrm{E}}(\alpha)=-\frac{1}{\sqrt{2\mu}}\left(\frac{K}{S_0}\right)^{\frac{\varpi+\sigma-\sqrt{2\mu}}{\sigma}}\frac{1}{\varpi+\sigma-\sqrt{2\mu}}.$$

Since the derivation of the formula is not found in the literature to the best of the authors' knowledge, we present its brief proof.

**Derivation of $\widehat{\Delta}(\alpha)$ when $S_0<L$:** Again by changing the order of differentiation and integration, we compute the Laplace transform of the delta when $S_0<L$ as follows:

$$\begin{aligned}&\widehat{\Delta}(\alpha)\\ &=\frac{\partial\widehat{\mathfrak{C}}^{\mathrm{E}}(\alpha)}{\partial S_0}+\frac{e^{\varpi b}}{\sigma S_0}\left(\widehat{\mathfrak{C}}\left(\alpha;L,D\right)-\widehat{\mathfrak{C}}^{\mathrm{E}}(\alpha;L)\right)\int_0^d e^{-\mu u}\left(-\varpi-\frac{1}{b}+\frac{b}{u}\right)\mu_b(\mathrm{d}u).\end{aligned}$$

We need to compute $\int_0^d e^{-\mu u}(b/u)\mu_b(\mathrm{d}u)$. Adopting the procedure described in Labart and Lelong [2009], we apply changes of variables, first $t=\sqrt{b}/\sqrt{\xi u}$ and second $v=1/t-t$ where $\xi=\sqrt{2\mu}$, and obtain

$$\int_0^d e^{-\mu u}\frac{b}{u}\mu_b(\mathrm{d}u)=\sqrt{\frac{b\xi}{2\pi}}e^{-\xi b}\int_{-\infty}^{\sqrt{\frac{\xi d}{b}}-\sqrt{\frac{b}{\xi d}}}e^{-\xi b v^2/2}g(v)\mathrm{d}v$$

where $g(v)=\xi(1+v^2)-\xi(3+v^2)v/\sqrt{v^2+4}$. One last change of variable is made to get a simpler integral. With $u=\sqrt{\xi b}v$,

$$\begin{aligned}\int_0^d e^{-\mu u}\frac{b}{u}\mu_b(\mathrm{d}u)&=e^{-\xi b}\int_{-\infty}^{\alpha}\phi(u)\left(\xi+\frac{u^2}{b}\right)\mathrm{d}u-e^{-\xi b}\int_{-\infty}^{\alpha}\phi(u)\left(3\xi+\frac{u^2}{b}\right)\frac{u}{\sqrt{u^2+4\xi b}}\mathrm{d}u\\ &=e^{-\xi b}\int_{-\infty}^{\alpha}\phi(u)\left(\xi+\frac{u^2}{b}\right)\mathrm{d}u+e^{\xi b}\int_{-\infty}^{\beta}\phi(u)\left(-\xi+\frac{u^2}{b}\right)\mathrm{d}u.\end{aligned}$$

Here, two new constants are defined: $\alpha=\xi\sqrt{d}-b/\sqrt{d}$ and $\beta=-\xi\sqrt{d}-b/\sqrt{d}$. Utilizing $\int_{-\infty}^{x}\phi(u)u^2\mathrm{d}u=\Phi(x)-x\phi(x)$ and (1), direct calculations yield

$$\begin{aligned}\int_0^d e^{-\mu u}\left(-\varpi-\frac{1}{b}+\frac{b}{u}\right)\mu_b(\mathrm{d}u)&=\frac{1}{\sqrt{d}}\left(e^{-\xi b}\phi(\alpha)+e^{\xi b}\phi(\beta)\right)\\ &\quad+e^{-\xi b}(\xi-\varpi)\Phi(\alpha)-e^{\xi b}(\xi+\varpi)\Phi(\beta)\end{aligned}$$

from which the final expression is easily derived. ■

### B.3 Parisian theta

For the sensitivity of the option price with respect to time, we recall that $S_0 > L$ is simple because there is no excursion. Indeed, straightforward computations yield

$$\widehat{\theta}(\alpha) = -\alpha\widehat{\mathfrak{C}}(\alpha).$$

In contrast, the case $S_0 \leq L$ with the remaining window $d$ is a bit more involved since we need to incorporate the sensitivity with respect to time-to-maturity as well as the sensitivity with respect to the excursion $d$. Hence, by considering $\partial\mathfrak{C}/\partial\tau$ with $\tau = T - t$ and $\partial\mathfrak{C}/\partial d$ together, it is not difficult to see that

$$\widehat{\theta}(\alpha) = -\alpha\widehat{\mathfrak{C}}(\alpha) - \left(\widehat{\mathfrak{C}}(\alpha; L, D) - \widehat{\mathfrak{C}}^{\mathrm{E}}(\alpha; L)\right) \frac{be^{\varpi b - \mu d - b^2/(2d)}}{\sqrt{2\pi d^3}}.$$

## C Vanilla Options and Binary Options under a Jump-diffusion Dynamics

In this last section, we compute European call and put options using Laplace transforms for consistency. This is contrasted with the approach in Kou [2002]. Utilizing the solution method in Albrecher et al. [2012], we observe that

$$\begin{aligned}
\widehat{\mathfrak{C}}^{\mathrm{E}}(\alpha) &= \int_0^\infty e^{-\alpha T}\mathfrak{C}_0^{\mathrm{E}}(S_0; T, K)\mathrm{d}T \\
&= \int_0^\infty \int_{-\infty}^\infty e^{-(\alpha+r)T}(e^y - K)^+ \mathsf{P}^x(X_T \in \mathrm{d}y)\mathrm{d}T \\
&= \int_0^\infty \int_{-\infty}^\infty e^{-(\alpha+r)T} e^x (e^{y-x} - Ke^{-x})^+ \mathsf{P}^0(X_T \in \mathrm{d}(y-x))\mathrm{d}T \\
&= \int_{-\infty}^\infty e^x \left(e^u - Ke^{-x}\right)^+ \mathsf{P}^0\left(X_{e_{\alpha+r}} \in \mathrm{d}u\right) \frac{\mathrm{d}u}{\alpha + r} \\
&= \int_{-\infty}^\infty e^x \left(e^u - Ke^{-x}\right)^+ p_{\alpha+r}(u)\mathrm{d}u
\end{aligned}$$

where $\widehat{\mathfrak{C}}^{\mathrm{E}}(\alpha)$ is the Laplace transform of a European call with initial price $S_0 = e^x$, strike $K$, and risk-free rate $r$. Here $p_{\alpha+r}(u)$ is the function defined in p.113 of Albrecher et al. [2012].

Then, we further proceed as

$$\begin{aligned}
\widehat{\mathfrak{C}}^{\mathrm{E}}(\alpha) &= \int_{-\infty}^\infty (e^y - K)^+ p_{\alpha+r}(y-x)\mathrm{d}y \\
&= \int_x^\infty (e^y - K)^+ p_{\alpha+r}(y-x)\mathrm{d}y + \int_{-\infty}^x (e^y - K)^+ p_{\alpha+r}(y-x)\mathrm{d}y \\
&= \int_x^\infty C_1^{\alpha+r} e^{-\beta_1^{\alpha+r}(y-x)} (e^y - K)^+ \mathrm{d}y + \int_x^\infty C_2^{\alpha+r} e^{-\beta_2^{\alpha+r}(y-x)} (e^y - K)^+ \mathrm{d}y \\
&\quad + \int_{-\infty}^x C_3^{\alpha+r} e^{\beta_3^{\alpha+r}(y-x)} (e^y - K)^+ \mathrm{d}y + \int_{-\infty}^x C_4^{\alpha+r} e^{\beta_4^{\alpha+r}(y-x)} (e^y - K)^+ \mathrm{d}y
\end{aligned}$$

$$= \sum_{i=1}^{2} J_3(C_i^{r+\alpha}, \beta_i^{r+\alpha}, x, K) + \sum_{i=3}^{4} J_4(C_i^{r+\alpha}, \beta_i^{r+\alpha}, x, K).$$

The put price is easily obtained via the put-call parity:

$$\mathfrak{P}_0^{\mathrm{E}}(S_0; T, K) = \mathfrak{C}_0^{\mathrm{E}}(S_0; T, K) + Ke^{-rT} - S_0.$$

As for the binary call, we apply similar arguments and get

$$\begin{aligned}
\widehat{\mathfrak{C}}^{\mathrm{bin}}(\alpha) &= \int_0^\infty e^{-\alpha T} \mathfrak{C}_0^{\mathrm{bin}}(S_0; T, K) \mathrm{d}T \\
&= \int_{-\infty}^{\infty} \mathbf{1}_{\{e^y > K\}} p_{\alpha+r}(y - x) \mathrm{d}y \\
&= \int_x^\infty C_1^{\alpha+r} e^{-\beta_1^{\alpha+r}(y-x)} \mathbf{1}_{\{e^y > K\}} \mathrm{d}y + \int_x^\infty C_2^{\alpha+r} e^{-\beta_2^{\alpha+r}(y-x)} \mathbf{1}_{\{e^y > K\}} \mathrm{d}y \\
&\quad + \int_{-\infty}^x C_3^{\alpha+r} e^{\beta_3^{\alpha+r}(y-x)} \mathbf{1}_{\{e^y > K\}} \mathrm{d}y + \int_{-\infty}^x C_4^{\alpha+r} e^{\beta_4^{\alpha+r}(y-x)} \mathbf{1}_{\{e^y > K\}} \mathrm{d}y.
\end{aligned}$$

If $S_0 = e^x < K$, then the computation reduces to

$$\widehat{\mathfrak{C}}^{\mathrm{bin}}(\alpha) = \frac{C_1^{\alpha+r}}{\beta_1^{\alpha+r}} \left(\frac{S_0}{K}\right)^{\beta_1^{\alpha+r}} + \frac{C_2^{\alpha+r}}{\beta_2^{\alpha+r}} \left(\frac{S_0}{K}\right)^{\beta_2^{\alpha+r}}.$$

If $S_0 = e^x \geq K$, then

$$\widehat{\mathfrak{C}}^{\mathrm{bin}}(\alpha) = \frac{C_1^{\alpha+r}}{\beta_1^{\alpha+r}} + \frac{C_2^{\alpha+r}}{\beta_2^{\alpha+r}} + \frac{C_3^{\alpha+r}}{\beta_3^{\alpha+r}} \left[1 - \left(\frac{K}{S_0}\right)^{\beta_3^{\alpha+r}}\right] + \frac{C_4^{\alpha+r}}{\beta_4^{\alpha+r}} \left[1 - \left(\frac{K}{S_0}\right)^{\beta_4^{\alpha+r}}\right].$$